

STATE OF ALASKA
DEPARTMENT OF NATURAL RESOURCES
DIVISION OF GEOLOGICAL AND GEOPHYSICAL SURVEYS

STATE OF ALASKA

Bill Sheffield, *Governor*

Esther C. Wunnicke, *Commissioner, Dept. of Natural Resources*

Ross G. Schaff, *State Geologist*

December 1984

Report of Investigations 84-26
LIQUEFACTION-SUSCEPTIBILITY ANALYSIS FOR
FOUNDATION SOILS, KNIK RIVER BRIDGE,
GLENN HIGHWAY, ALASKA
by
Randall G. Updike
In cooperation with the
U.S. Geological Survey
Office of Earthquake Studies

STATE OF ALASKA
Department of Natural Resources
DIVISION OF GEOLOGICAL & GEOPHYSICAL SURVEYS

According to Alaska Statute 41, the Alaska Division of Geological and Geophysical Surveys is charged with conducting 'geological and geophysical surveys to determine the potential of Alaska lands for production of metals, minerals, fuels, and geothermal resources; the locations and supplies of ground waters and construction materials; the potential geologic hazards to buildings, roads, bridges, and other installations and structures; and shall conduct other surveys and investigations as will advance knowledge of the geology of Alaska.'

In addition, the Division shall collect, evaluate, and publish data on the underground, surface, and coastal waters of the state. It shall also file data from water-well-drilling logs.

DGGS performs numerous functions, all under the direction of the State Geologist---resource investigations (including mineral, petroleum, and water resources), geologic-hazard and geochemical investigations, and information services.

Administrative functions are performed under the direction of the State Geologist, who maintains his office in Anchorage (ph. 276-2653).

This report is for sale by DGGS for \$2. It may be inspected at the following locations: Alaska National Bank of the North Bldg., Geist Rd. and University Ave., Fairbanks; 3601 C St. (10th floor), Anchorage; 400 Willoughby Center (3rd floor), Juneau; and the State Office Bldg., Ketchikan.

Mail orders should be addressed to DGGS, 794 University Ave. (Basement), Fairbanks 99701.

CONTENTS

| | <u>Page</u> |
|---|-------------|
| Abstract..... | 1 |
| Introduction..... | 1 |
| Location and geologic setting..... | 3 |
| Data acquisition..... | 5 |
| Cone-penetration testing program..... | 6 |
| Equipment and field methods..... | 6 |
| Data reduction and interpretation..... | 6 |
| Testing results..... | 8 |
| Liquefaction-susceptibility analyses..... | 10 |
| General comments..... | 10 |
| Historic observations..... | 14 |
| Assessment of borehole logs..... | 15 |
| Standard-penetration-test evaluation..... | 21 |
| Quantitative assessment..... | 21 |
| Conclusions..... | 23 |
| Acknowledgments..... | 25 |
| References cited..... | 25 |
| Appendix A - Tabulated data for cone-penetration-test soundings at the Knik River bridge, new Glenn Highway, Alaska..... | 28 |
| Appendix B - Equations used for calculations..... | 33 |

FIGURES

| | |
|---|----|
| Figure 1. Location map of study area, upper Knik Arm area, south- central Alaska..... | 2 |
| 2. Oblique aerial view of the Knik River bridge, new Glenn Highway, Alaska..... | 3 |
| 3. Aerial view of an active segment of the Border Ranges fault system..... | 4 |
| 4. Regional view of the Knik River bridge and the Knik River flood plain..... | 5 |
| 5. Map showing the location of the Knik River bridge and points of subsurface-data acquisition..... | 7 |
| 6. Electric-cone-penetration-test laboratory truck with hydraulic jacks extended before initiating sounding.... | 8 |
| 7. Cone-penetration-test probe in position to initiate sounding..... | 9 |
| 8. Cone-penetration-test probe with disassembled conical tip and friction sleeve..... | 10 |
| 9. Cross-section of CPT instrument package used in this study. | 11 |
| 10. Cone-penetration-test sounding log for site KR-1..... | 12 |
| 11. Cone-penetration-test sounding log for site KR-2..... | 13 |
| 12. Cone-penetration-test sounding log for site KR-3..... | 14 |
| 13. Cone-penetration-test sounding log for site KR-4..... | 15 |
| 14. Soil-classification chart used for prediction of soil- behavior types tabulated in appendix A..... | 16 |
| 15. Example of computer tracking of selected intervals of CPT soundings KR-1 and KR-4 in plot of friction ratio vs cone resistance..... | 17 |

| | <u>Page</u> |
|---|-------------|
| 16. Predicted SPT values vs depth for Knik River bridge, new Glenn Highway, using CPT data (KR-1, KR-2)..... | 18 |
| 17. Predicted SPT values vs depth for Knik River bridge, new Glenn Highway, using CPT data (KR-3, KR-4)..... | 19 |
| 18. Map of distribution of ground fissures in the Knik River flood plain that resulted from the 1964 earthquake..... | 20 |
| 19. Plot of standard-penetration test vs depth showing domains of liquefaction susceptibility..... | 22 |
| 20. Plot of modified SPT blow count (N_1) vs cyclic-stress ratio..... | 24 |

TABLE

| | |
|--|----|
| Table 1. Data calculations for liquefaction-susceptibility analyses. | 23 |
| 2. CPT log for sounding KR-1..... | 28 |
| 3. CPT log for sounding KR-2..... | 30 |
| 4. CPT log for sounding KR-3..... | 31 |
| 5. CPT log for sounding KR-4..... | 32 |

LIQUEFACTION-SUSCEPTIBILITY ANALYSIS FOR FOUNDATION SOILS,
KNIK RIVER BRIDGE, GLENN HIGHWAY, ALASKA

By
Randall G. Updike¹

ABSTRACT

The Knik River bridge, part of the new Glenn Highway 25 mi (40 km) north of Anchorage, is a critical transportation link to Palmer, Wasilla, and southern interior Alaska (fig. 1). Sediments on which the bridge is founded apparently failed during the 1964 Prince William Sound Earthquake. Four methods of liquefaction-susceptibility analyses were used to study the site: 1) historic observations, 2) examination of borehole and cone-penetration-test logs, 3) standard-penetration-test evaluation, and 4) state-of-the-art quantitative assessment. Results of these analyses indicate the soils that support the bridge piles will probably liquefy---in a lateral-spreading-type failure---during earthquakes with peak ground accelerations (g) of 0.3 g or greater. If this type of failure occurs, the continued integrity of the bridge is doubtful.

INTRODUCTION

Numerous highway and railroad bridges in Alaska were rendered unusable or were damaged by the 1964 Prince William Sound Earthquake. Liquefaction, although poorly understood at the time, was responsible for several bridge failures (McCulloch and Bonilla, 1970; Youd, 1978). Subsequent to 1964, additional research on the behavior of cohesionless soils during earthquake shaking significantly clarified our understanding of the liquefaction process, and substantial progress has been made in defining necessary boundary conditions (for instance, Seed, 1968, 1979; Seed and others, 1983; Casagrande, 1976; Bennett and others, 1981). The evaluation of liquefaction is now incorporated in seismic-safety-design criteria for construction projects throughout the world.

At the time of the 1964 earthquake, the new Glenn Highway across the Knik and Matanuska River flood plains was in the design and construction phases. The old Glenn Highway crossed the Knik River on a pier and steel truss bridge about 7.5 mi (12 km) upstream from the new Glenn Highway bridge. This was the only bridge on the old Glenn Highway to sustain severe damage during the earthquake; the cracking, canting, and displacement of concrete piers toward the center of the river indicate lateral spreading of foundation soils. Other nearby highway bridges built on bedrock (for instance, Peters Creek and Eklutna River) sustained slight to no damage (Kachadoorian, 1968). The Alaska Railroad bridge, constructed of steel girders on wood and steel piles, was subjected to compressional damage throughout its length, and individual piers were displaced up to 9 in. (23 cm). This bridge is approximately 1,700 ft (515 m) upstream from the new Glenn Highway bridge. Extensive ground fissures were mapped along the channel and on adjacent island uplands between the two bridge locations (McCulloch and Bonilla,

¹DGGS, P.O. Box 772116, Eagle River, Alaska 99577.

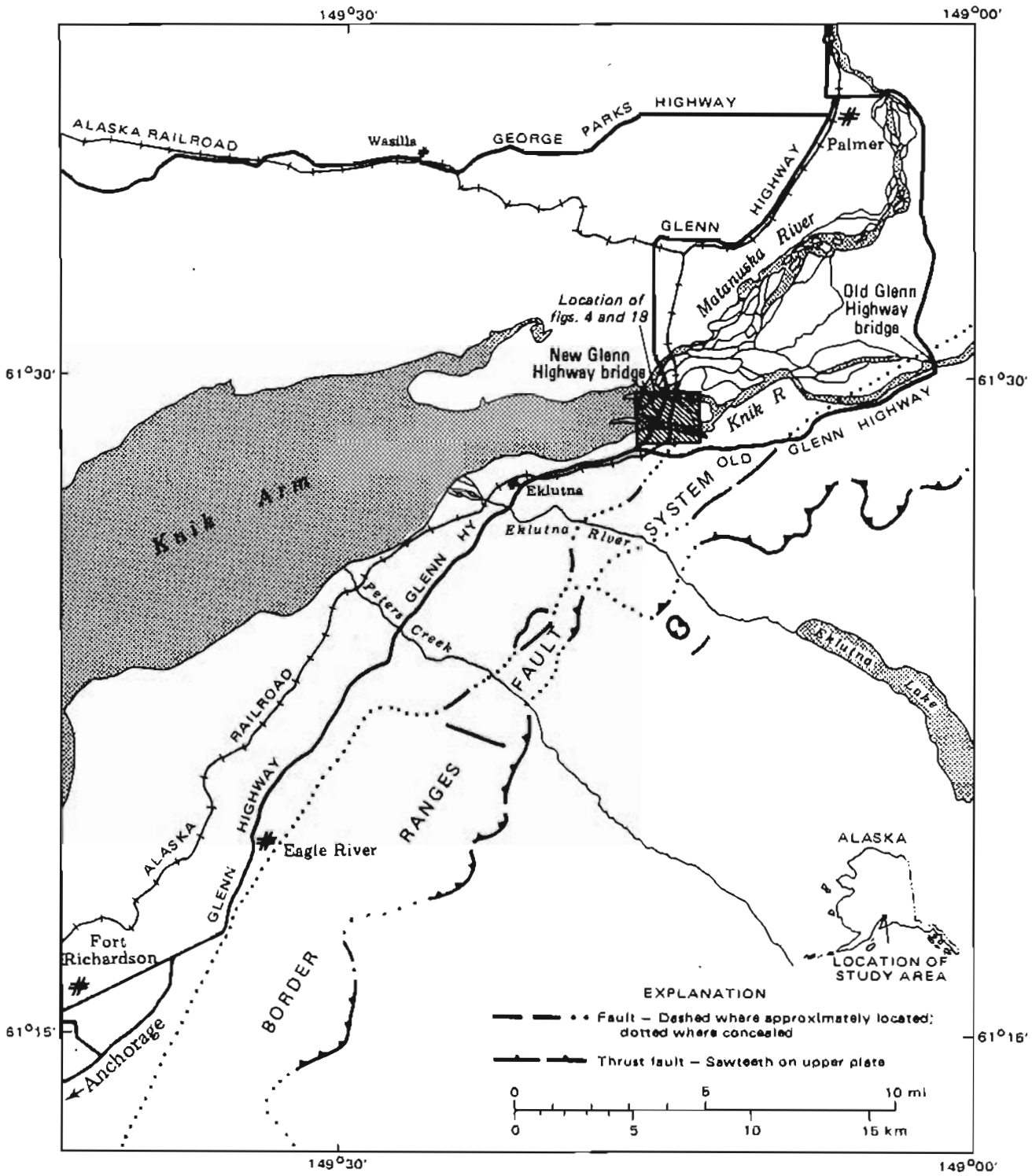


Figure 1. Location map of study area, upper Knik Arm area, south-central Alaska.

1970). The evidence indicates that the subsidence and horizontal displacements that occurred in sediments throughout the Knik River flood plain during the earthquake affected the integrity of the bridges.

The new Glenn Highway Knik River bridge (fig. 2) is a critical link in the highway corridor leading north to the interior of the State. Within the design life of the structure, major seismic events related to the underlying subduction zone or the nearby Border Ranges fault system, which shows



Figure 2. Oblique aerial view (looking south) of the Knik River bridge, new Glenn Highway, Alaska. The Alaska Railroad bridge is visible at upper left (1983).

evidence of activity in Holocene time (fig. 3), are anticipated. The bridge is a masonry and girder superstructure on piers over steel piles. The piles are driven into saturated, fine- to medium-grained, cohesionless soils. These factors promote substantial concern for the seismic safety of the bridge during its period of use and, in particular, warrant an evaluation of liquefaction susceptibility at the site.

LOCATION AND GEOLOGIC SETTING

The new Glenn Highway Knik River bridge is located near the mouth of the Knik River, approximately 25 mi (40 km) north of Anchorage, in the NE $\frac{1}{4}$ sec. 15, T. 16 N., R. 1 E., of the Seward Meridian, Anchorage B-7NE Quadrangle (fig. 4).



Figure 3. Aerial view (looking south) of an active segment of the Border Ranges fault system (the Twin Peaks fault) that extends from left to right in the center of the photograph (Updike and Ulery, 1983). This locality is within 3.5 mi (6 km) of the Knik River bridge (1982).

The bridge is located on that part of the Knik River flood plain that is transitional to the estuarine environment of upper Knik Arm (upper Cook Inlet), and the river channel and adjacent lowlands are influenced diurnally by tides that encroach from Knik Arm. These tidal waters---and the river itself---transport large suspended and tractive loads of silt and sand. Within the active flood-plain regime, deposition and rapid scour seem to alternately dominate, but no firm data exist to confirm the long-term net affect of these processes. Post-1964 survey data indicate that this region of upper Cook Inlet subsided about 2 ft (0.7 km) as a result of the earthquake (Foster and Karlstrom, 1967), and that substantial subsequent uplift has occurred (Brown and others, 1977). The result of these sedimentary-basin fluctuations has caused relatively rapid fine-grained sediment aggradation during latest Holocene time. Most sediment exposed at or near the surface near the bridge is predominantly gray silt and sand. Highway borrow pits downstream and northwest of the bridge were sources of sand and gravel used for highway-construction fill. The coarser aggregate in the subsurface indicates that the Knik River formerly maintained a higher energy regime or lower base level. Sand and gravel that are presently exposed on the flood plain less than 3 mi (4.8 km) to the east are gradually buried by the silty sands downstream, where estuarine conditions prevail.



Figure 4. Regional view of the Knik River bridge (right center) and the Knik River flood plain. The Alaska Railroad bridge is directly upstream from the highway bridge, and Pioneer Peak is in the center background. The old Glenn Highway Knik River bridge is out of view beyond the left corner of Pioneer Peak. Most of the flood plain in this view was extensively fissured during the 1964 earthquake (1983).

The southeast approach to the bridge skirts a prominent butte of Mesozoic Peninsular terrane composed of metasedimentary and metavolcanic rocks. The western side of the butte was apparently deeply eroded by water and ice during previous glaciations, because no bedrock was found in either boreholes or cone-penetration soundings. During late Pleistocene time, the butte was scoured by glacial ice, which, combined with subsequent wave erosion, may account for the abrupt truncation of bedrock.

DATA ACQUISITION

To evaluate the liquefaction susceptibility of soils near the bridge, subsurface data on soil particle-size distribution, density, penetration resistance, natural moisture content, and ground-water depth are necessary. The Alaska Department of Transportation and Public Facilities (DOT-PF) provided the Knik River bridge-foundation report (Alaska Department of Transportation and Public Facilities, 1963a) and the materials-site report (Alaska Department of Transportation and Public Facilities, 1963b), which

contain borehole logs and supporting laboratory data for 25 holes. The locations of these boreholes are given in figure 5.

Because moisture loss and sample disturbance may occur during borehole sampling and laboratory testing of noncohesive soils, in-situ testing is the most economical method of data acquisition in liquefaction studies. Penetration testing is the approach most universally used and is based on the concept that the force or energy required to push or drive a standardized probe into the soil can be translated into a measure of liquefaction susceptibility. Principal penetration methods include the standard-penetration test (SPT) and the cone-penetration test (CPT). The SPT has been used for many years and remains a standard for various foundation-design needs of the geotechnical industry. The test consists of driving a 2.0 in.-diam (50.8 mm) split-spoon sampler into the soil by dropping a 140-lb (63 kg) mass from a height of 30 in. (760 mm). The penetration resistance (N) is reported in number of blows to drive the sampler 1.0 ft (305 mm). Although some significant variability of recorded values can occur based upon technique and testing conditions (see Gibbs and Holtz, 1957; McLean and others, 1975; Marcuson and Bieganousky, 1976), the SPT test remains the most universally applied test for liquefaction susceptibility.

Although the CPT method has been used in Europe for several years, the method has attained only recent acceptance by the United States geotechnical industry. The system used in this study has been used for a variety of major projects in the contiguous United States (for instance, nuclear-power sites, dams, pipeline corridors, and missile sites), but has not previously been used in Alaska.

CONE-PENETRATION TESTING PROGRAM

Equipment and Field Methods

The cone-penetration test (CPT) consists of pushing an instrumented, cone-tipped probe into the soil and continuously recording the soil's resistance to penetration. The tests were conducted in accordance with American Society for Testing and Materials specifications (ASTM-D3441-79) using an electric-cone penetrometer. The test equipment consists of a cone assembly, a series of hollow sounding rods, a hydraulic frame to push the cone and rods into the soil, an analog strip-chart recorder, and a truck to transport the test equipment and provide the needed 20-ton thrust-reaction capacity (fig. 6). The cone penetrometer (figs. 7 and 8) consists of a conical tip with a 60° apex angle and a cylindrical friction sleeve above the tip. The cone assembly used on this project has a cross-sectional area of 2.32 in.² (15 cm²) and a sleeve-surface area of 31 in.² (200 cm²). The device's interior (fig. 9) is instrumented with strain gauges that allow simultaneous measurement of cone and sleeve resistance during penetration. Continuous electric signals from the strain gauges are transmitted by cable in the sounding rods to the recorder at ground surface.

Data Reduction and Interpretation

Reduction of the CPT data involved the digitization of field strip-chart

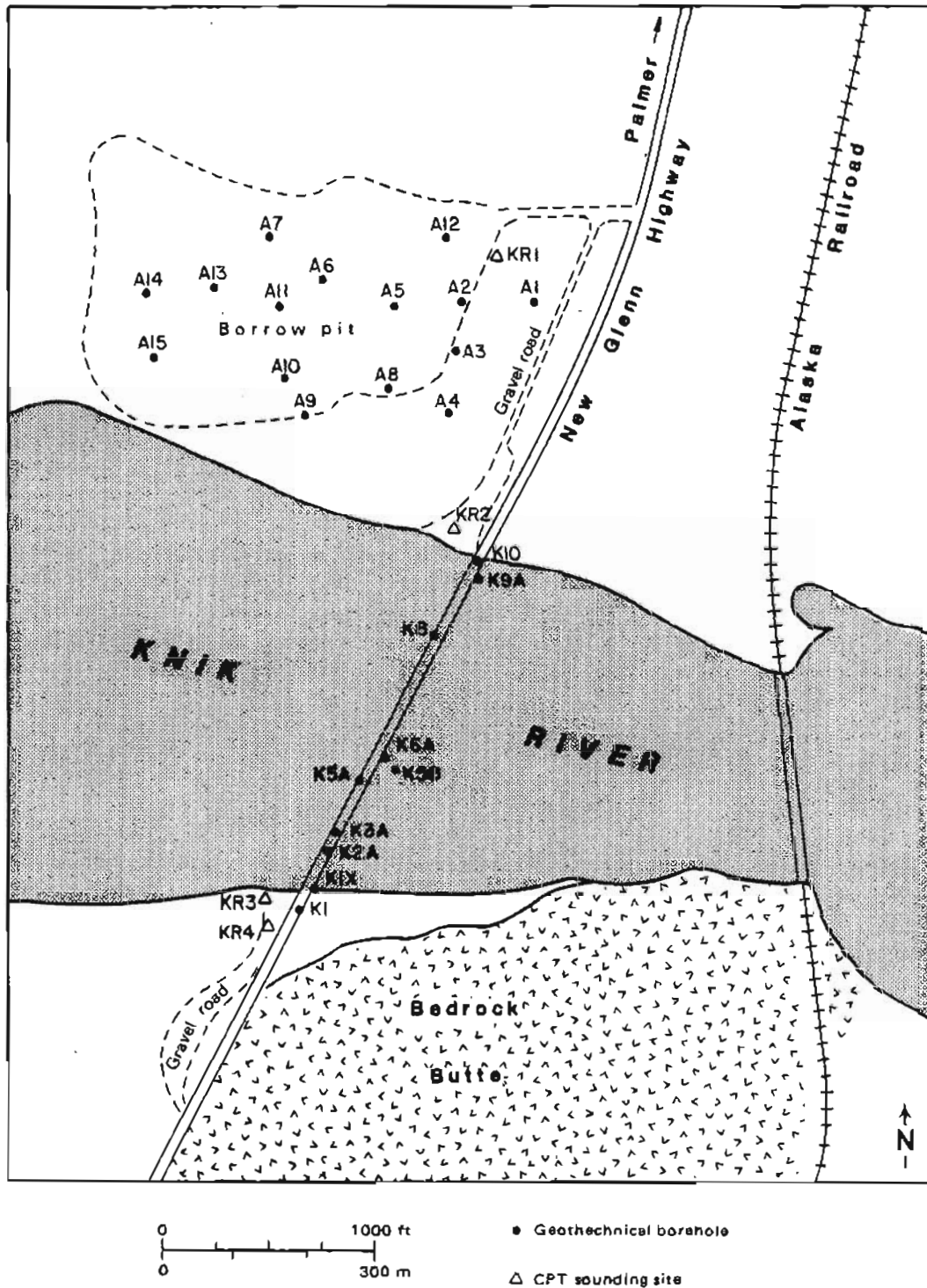


Figure 5. Map showing the location of the Knik River bridge and points of subsurface-data acquisition. Points with 'A' prefix are construction-materials-site borings, points with 'K' prefix are foundation-investigation borings, and KR triangles are cone-penetration-test sites.



Figure 6. Electric-cone-penetration-test laboratory truck with hydraulic jacks extended before initiating sounding (1982).

recordings and subsequent computer processing. Processing was done at the data-processing center of Earth Technology Corporation (Ertec), Long Beach, California. In addition to field-data reduction, subroutines that evaluated CPT soil-behavior types, equivalent SPT blow counts, and cone resistance vs friction ratio for selected depth intervals were performed. Bruce Douglas (Ertec Research Project Engineer), Brenda Meyer (Ertec Civil Engineer), and I interpreted the field data (CPT and adjacent borehole logs) for input into computer programs.

Testing Results

Four CPT soundings that were made at the Knik River bridge on April 9, 1982, ranged in total depth from 59 ft (17.8 m) to 109 ft (33 m). The resultant soundings (figs. 10-13) include the friction resistance (sleeve friction, f_s , in ton/ft²), cone resistance (end bearing, q_c , in ton/ft²), and friction ratio ($R_f = f_s/q_c$).

CPT soil-behavior predictions are tabulated in appendix A. The Ertec computer program estimates soil types by tracking the cone-end bearing and average friction ratio at each requested depth based on guidelines of a classification chart (fig. 14) that evolved from the work of Begemann (1965),

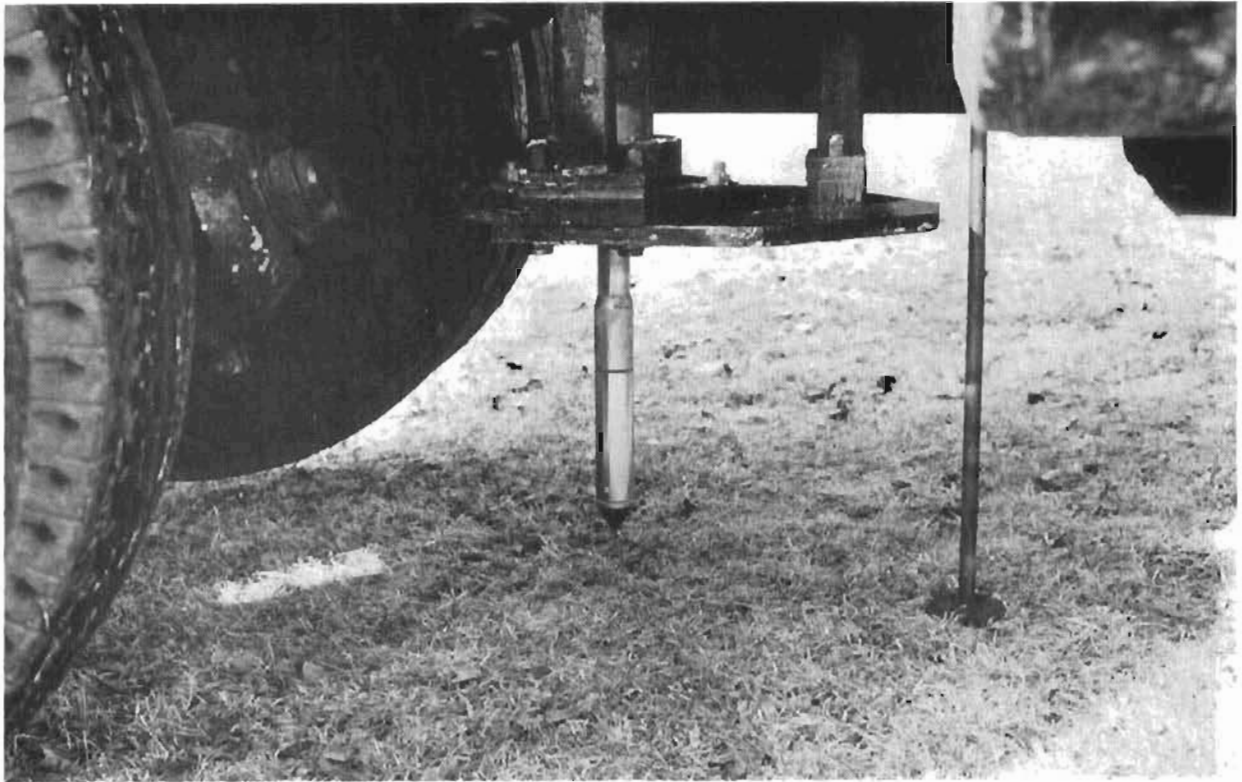


Figure 7. Cone-penetration-test probe in position to initiate sounding. Rod at right is used to calibrate distance between truck and ground level during sounding (1982).

Schmertmann (1971), Sanglerat (1972), and Searle (1979). The chart was calibrated to project equipment by Douglas and Olsen (1981). An example of the computer tracking for certain intervals in three soundings is shown in figure 15. Correlation of the computer trackings to the classification chart is the basis for the predicted soil-behavior types tabulated in appendix A.

As previously mentioned, the standard-penetration test is the commonly used method for assessing in-situ soil conditions. Currently, the resultant N values are used as a basis for liquefaction-potential analyses throughout the United States. Bennett and others (1981) and Douglas and others (1981) have successfully correlated penetration data derived from CPT and SPT techniques at a given site. The mathematical derivation of this correlation, which is beyond the scope of this report, is explained in Douglas and others (1981). From the relationships derived in that report, a computer program was designed using the CPT logs of the four sites, and the computer generated a predicted equivalent SPT profile for each site (figs. 16 and 17). Although actual SPT values are obtained with a sampler and therefore can only record a series of vertical data points with intervening data gaps, the CPT-equivalent technique provides a continuous predicted SPT profile with respect to depth. All SPT predictions were performed using the following equation:



Figure 8. Cone-penetration-test probe with disassembled conical tip and friction sleeve (1982).

$$N = 12.5 E_D^{1.3}$$

where N is the predicted blow count and E_D is the energy expended during soil penetration of the SPT sampler. Evaluation of the constants that relate the energy-dissipation function (E_D) to the SPT values in carefully monitored borings shows a good correlation between predicted and real SPT values using a low-energy, trip-hammer technique. This correlation of the profiles in figures 16 and 17 is most applicable to the liquefaction-potential analyses of noncohesive soils based upon the trip-hammer, SPT method. The constants relating N and E_D depend on the energy-transfer efficiency of the specific SPT hammer-anvil-rod-sampler system used. If the SPT data that uses some other system is correlated with the curves in figures 16 and 17, a conversion factor may be required. This calibration of measured and predicted SPT values specific to equipment has been successfully used by Douglas and others (1981).

LIQUEFACTION-SUSCEPTIBILITY ANALYSES

General Comments

The reader is encouraged to review recent literature on the mechanism of

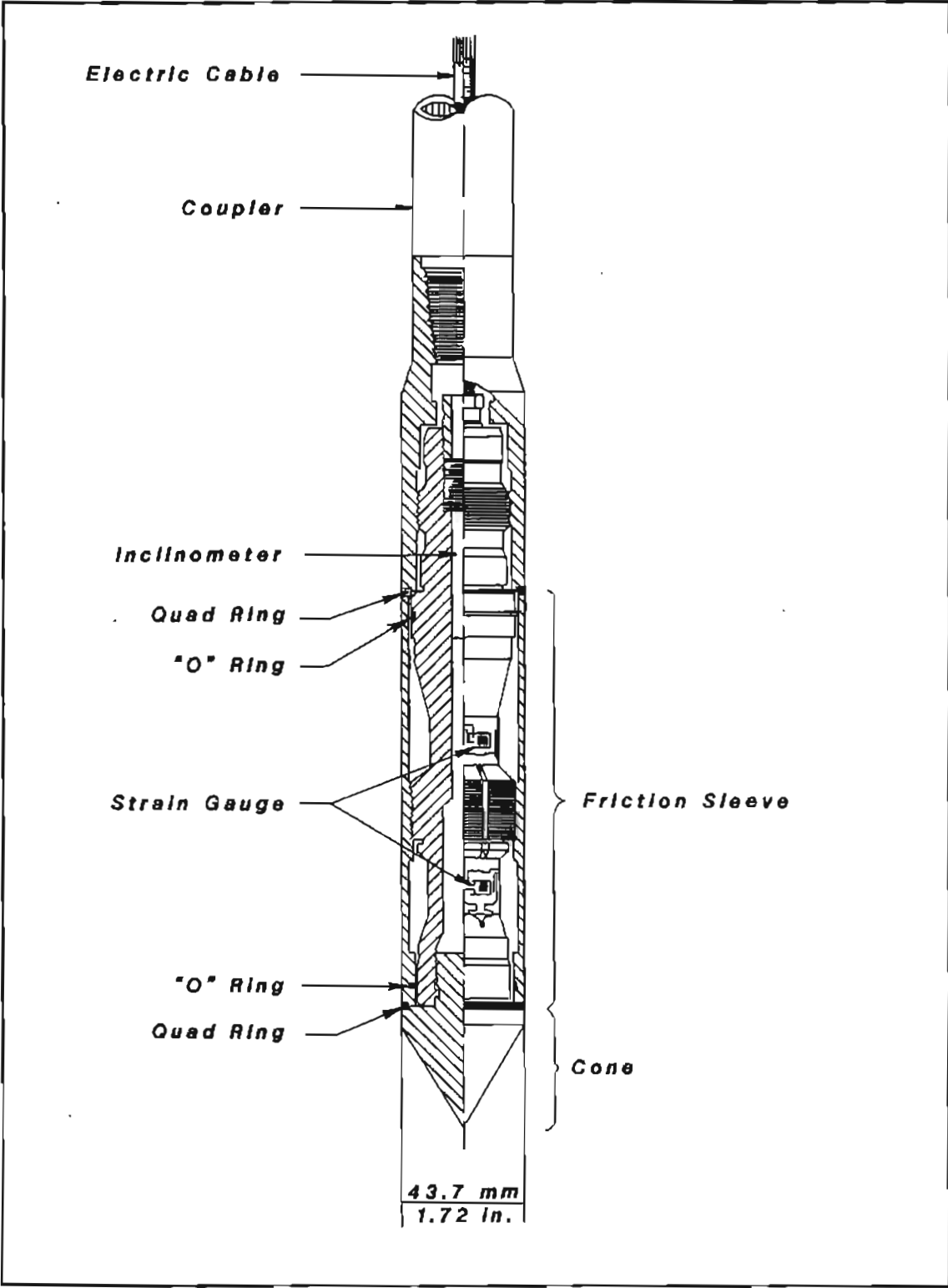


Figure 9. Cross section of CPT instrument package used in this study.

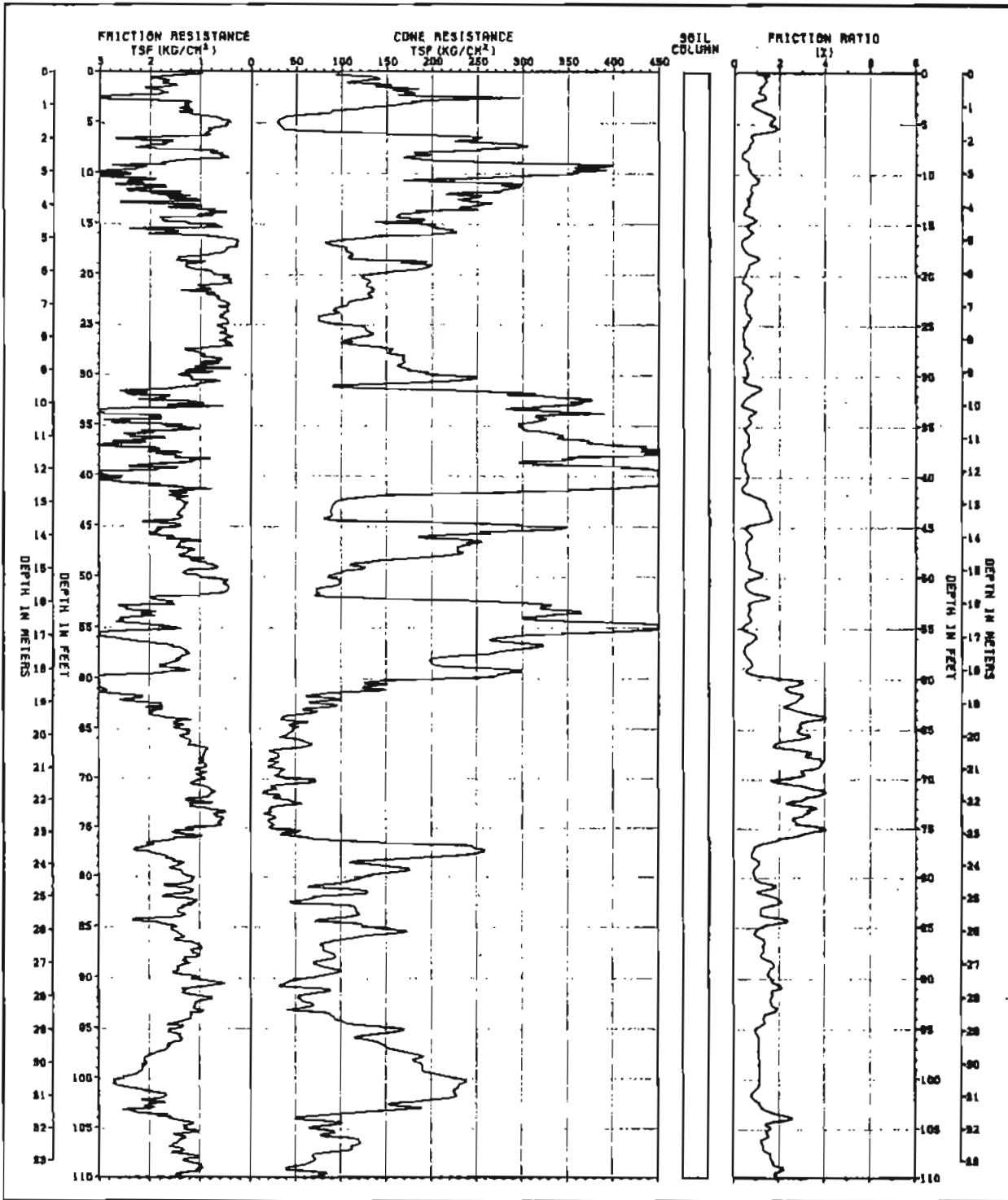


Figure 10. Cone-penetration-test sounding log for site KR-1.

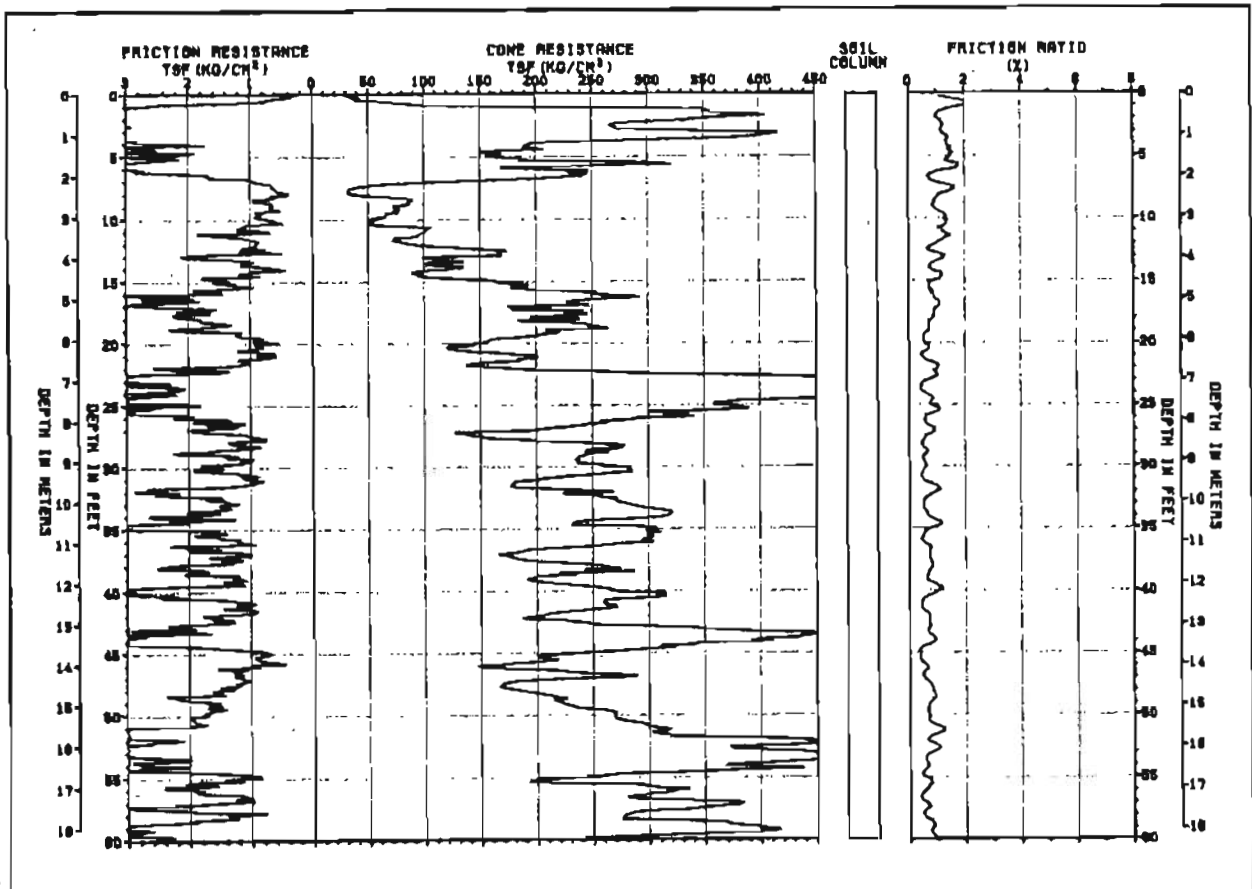


Figure 11. Cone-penetration-test sounding log for site KR-2.

seismically-induced liquefaction and current procedures for evaluation of liquefaction potential in noncohesive soils (Seed, 1976, 1979; Seed and others, 1983; Youd and Perkins, 1978; Bennett and others, 1981). Generally, these investigators agree that if a saturated, cohesionless soil (ideally a well-sorted sand or silty sand, but also some clayey sands and gravelly sands) is subjected to seismically-induced cyclic-shear stresses, the soil becomes more compact, with a resultant transfer of stress to the pore water and diminished stress on the soil particles. If cyclic stresses are sustained, a peak cyclic pore-pressure ratio of 100 percent---liquefaction---can be attained (Seed, 1979); if cyclic stress is continued, strain that results in 'cyclic mobility' may occur (Casagrande, 1976). Depending on the density of the sand, confining pressure, and magnitude of stress cycles, the soil may be mobilized to unlimited deformation or may sustain limited strain before dilating to a stable condition. The damage to structures built on or in these liquefied deposits can be severe (Ferritto and Forrest, 1977; Youd and Hoose, 1978). Bridges are particularly susceptible to severe damage due to lateral spread of foundation soils because spans are typically supported by piers constructed on poorly consolidated, noncohesive, saturated soils of the flood plain and adjacent terraces.

The assessment of liquefaction susceptibility of sedimentary units near the Knik River bridge is based on: 1) historic observations, 2) qualitative

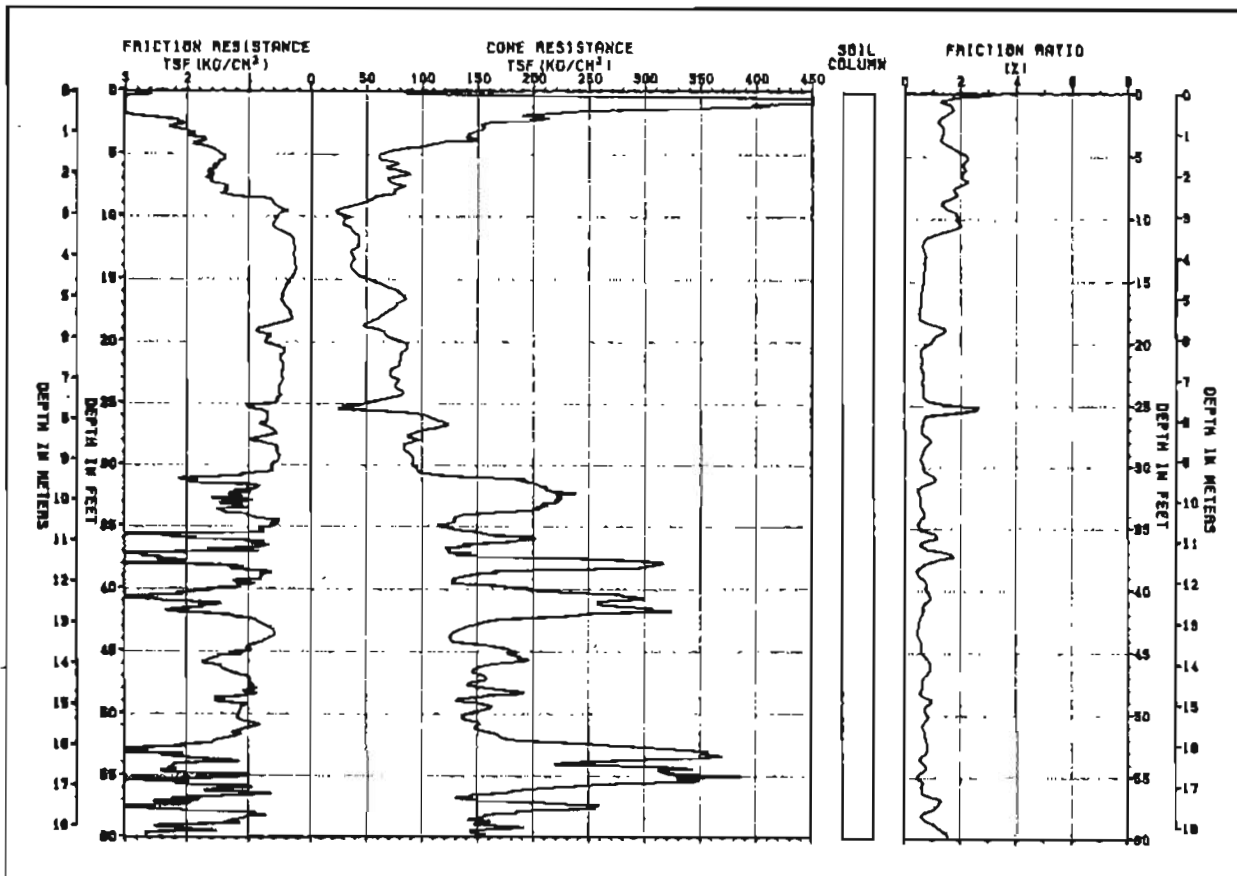


Figure 12. Cone-penetration-test sounding log for site KR-3.

assessment of borehole logs, 3) semiquantitative assessment of SPT and CPT data, and 4) quantitative assessment of field and laboratory data that have been used as indicators of performance of cohesionless soils in previous earthquakes.

Historic Observations

During the 1964 earthquake, substantial damage was sustained by both the Alaska Railroad bridge and the old Glenn Highway bridge that crossed the Knik River. In both cases, a primary mode of damage was compression caused by horizontal displacement of the supporting piers toward the center of the bridges. This displacement subjected the bridges to compressional forces that buckled the decks, sheared critical stress-point bolts, and canted the superstructures. In extreme cases, lateral stresses due to pier shifting can result in separation of the superstructure from the abutments and consequent collapse of deck spans.

Numerous ground fissures developed in the exposed flood plain of the Knik River (McCulloch and Bonilla, 1970; fig. 18) and, to a lesser degree, on the adjacent uplands. The configuration of the fissures suggests that at least the surface sediments underwent liquefaction and lateral spreading; data on the depth of failure were not available.

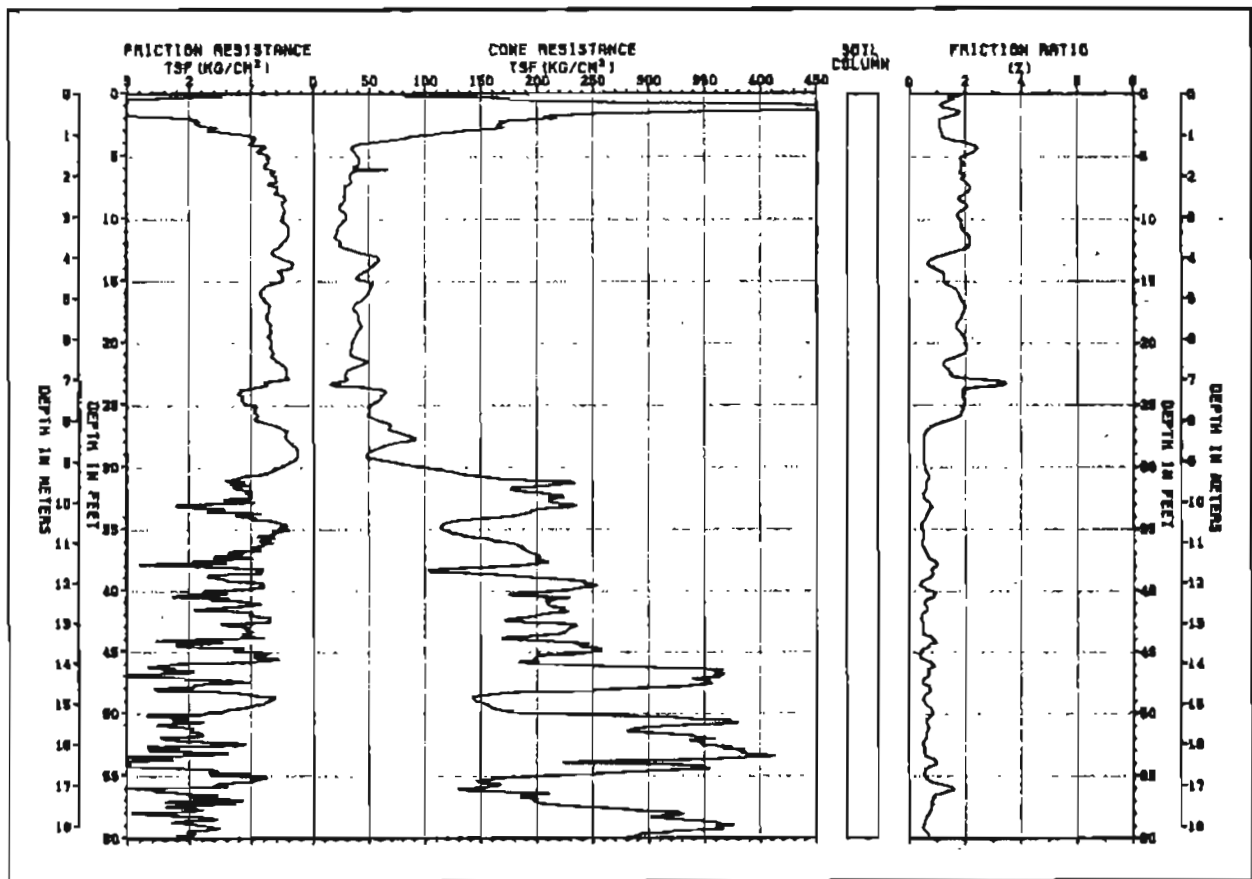


Figure 13. Cone-penetration-test sounding log for site KR-4.

Assessment of Borehole Logs

A preliminary, qualitative evaluation of liquefaction susceptibility can be made on the basis of interpretation of field data acquired from boreholes. Sherif and Ishibashi (1978) provide a flow chart for evaluation of the liquefaction potential of cohesionless soils. Liquefaction is primarily a shallow-soil phenomena [less than 50 ft (15 m) deep]. Borehole data for DOT-PF Project Material Site 11-001-63, which is located directly northwest of the Knik River bridge (fig. 5), provide 15 logs to depths of 8 to 13 ft (1.5 to 3.9 m) (Alaska Department of Transportation and Public Facilities, 1963b). In 14 boreholes, sand and gravelly sand were found beneath a surface layer of silt 4 to 6 ft (1.3-1.8 m) thick. Generally, these sediments were saturated 8 to 10 ft (1.5 to 3.0 m) below the ground surface. Youd and Perkins (1978) identified late Holocene estuarine flood-plain deposits that are moderately to highly susceptible to liquefaction elsewhere in the world. Thus, based upon depth, texture, moisture content, and geology, the soils near the bridge are considered liquefiable to a depth of 13 ft (4 m).

Although logs in the foundation-study report (Alaska Department of Transportation and Public Facilities, 1963a) do not provide sufficient information to reach this conclusion, they often indicate interbedded, gray, loose to slightly compact to dense sand and gravel. The trends of SPT and

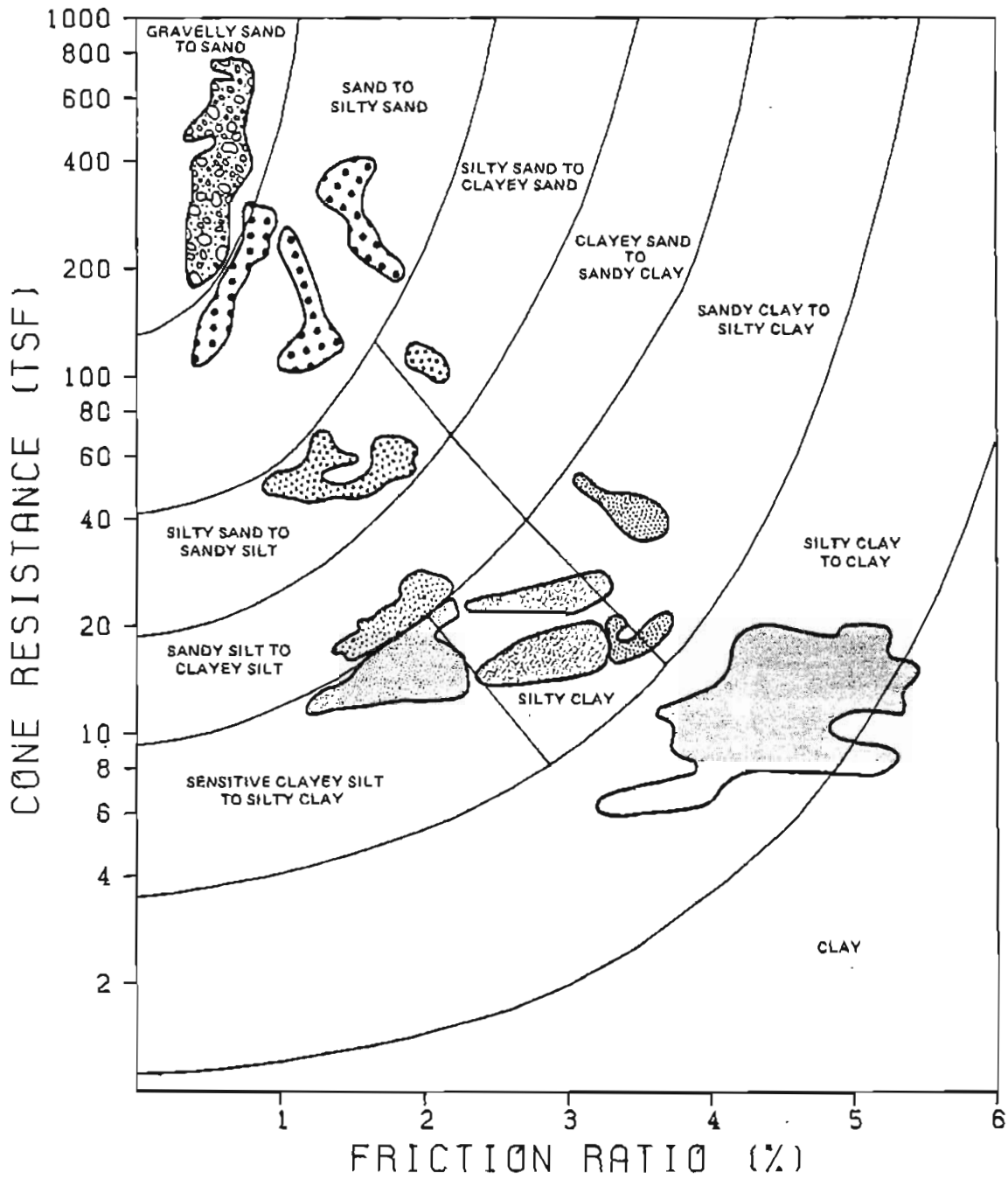


Figure 14. Soil-classification chart used for prediction of soil-behavior types tabulated in appendix A.

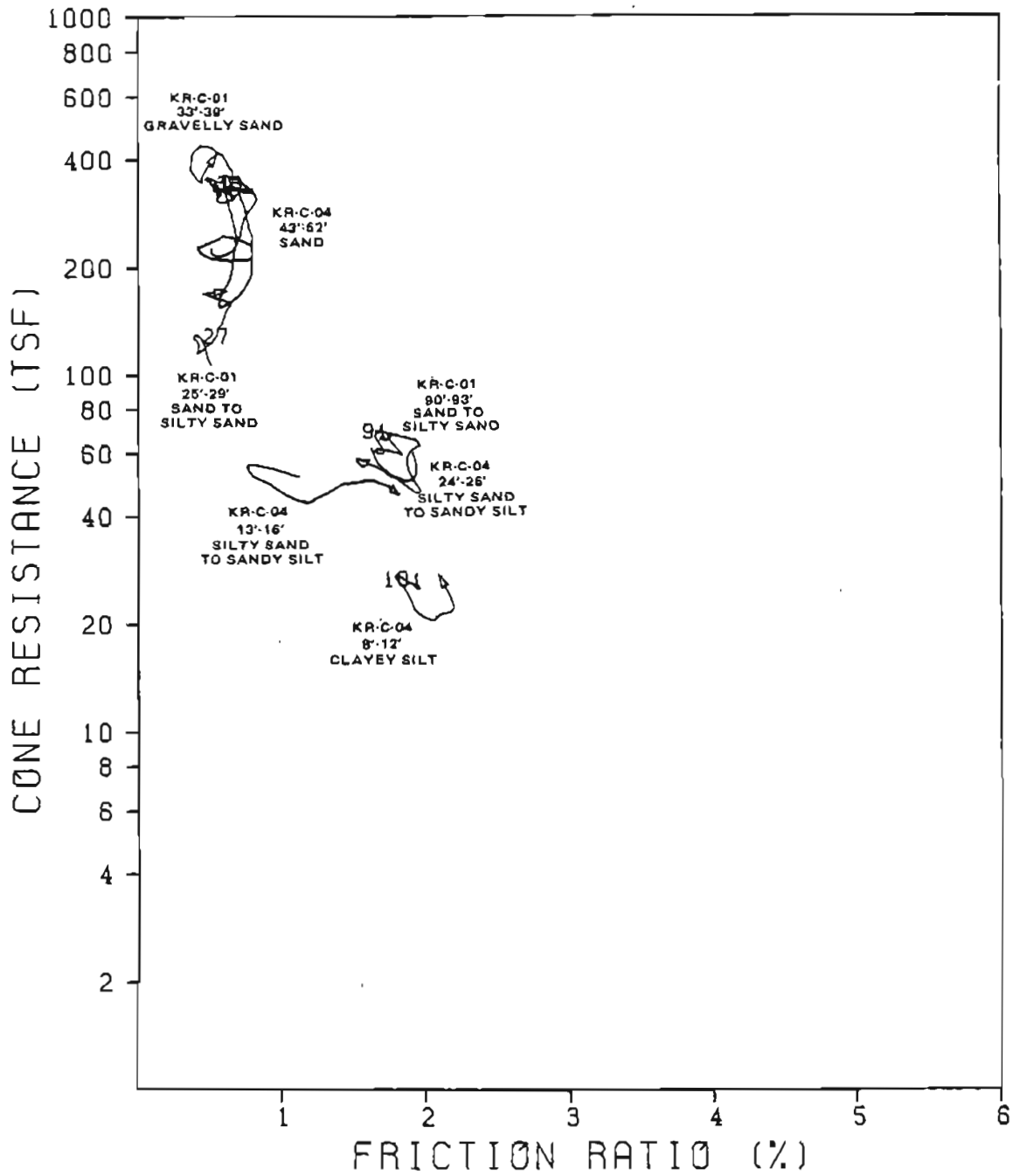


Figure 15. Example of computer tracking of selected intervals of CPT soundings KR-1 and KR-4 in plot of friction ratio vs cone resistance.

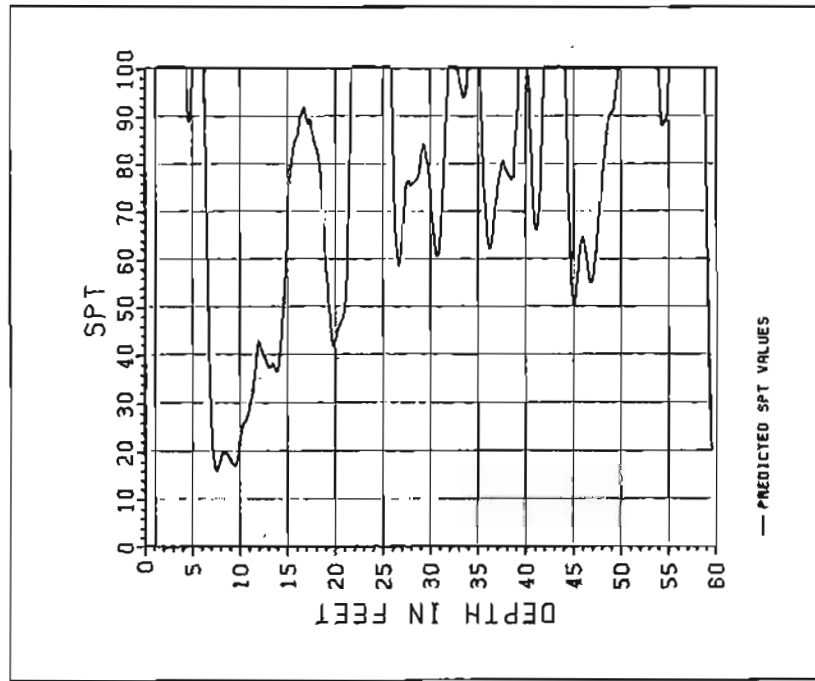
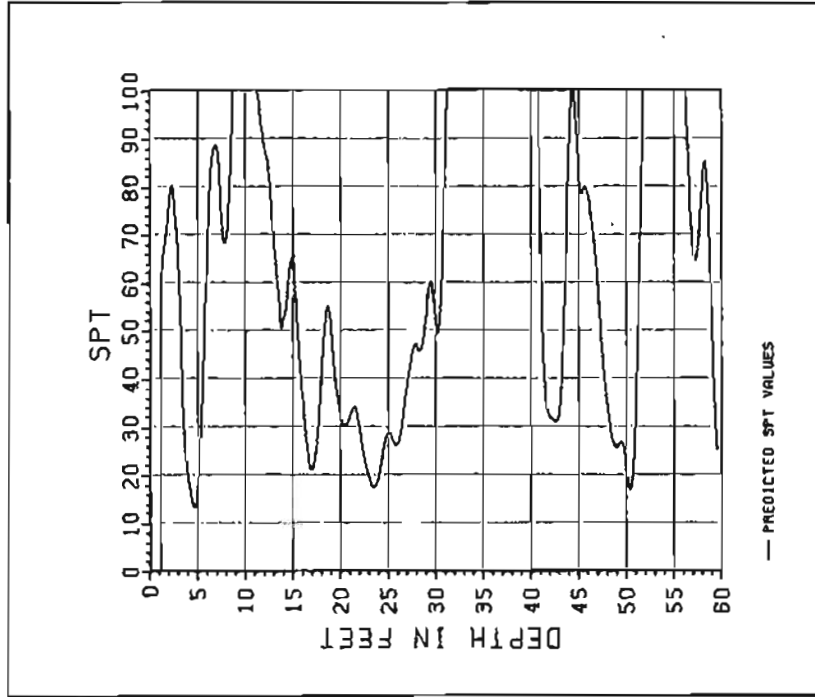


Figure 16. Predicted SPT values vs depth for Knik River bridge, new Glenn Highway, using CPT data. Sounding for KR-1 at right and for KR-2 at left.

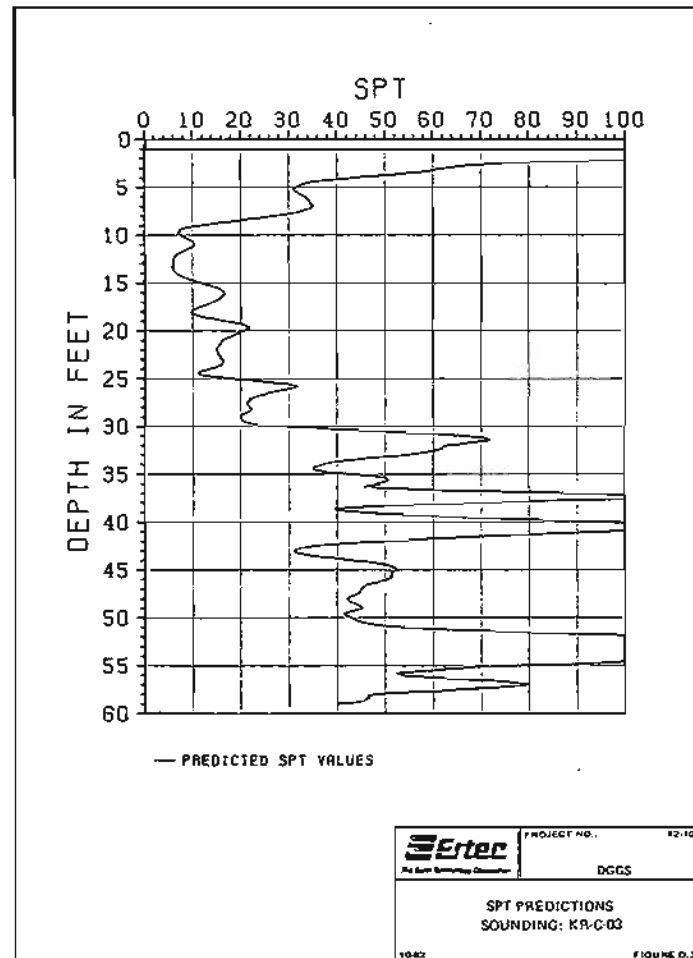
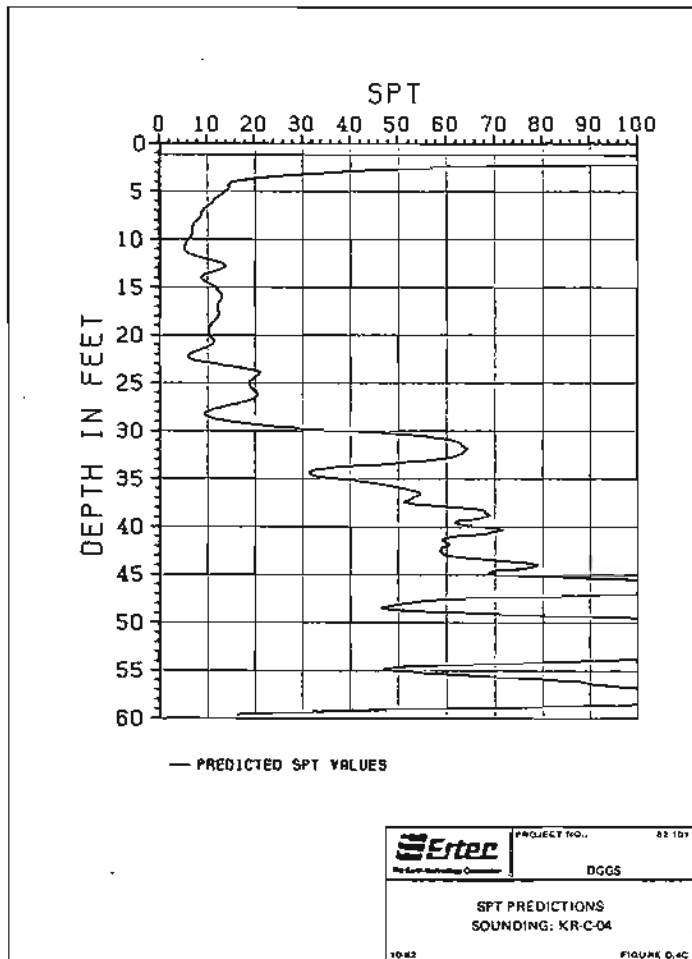


Figure 17. Predicted SPT values vs depth for Knik River bridge, new Glenn Highway, using CPT data. Sounding for KR-3 at right and KR-4 at left.

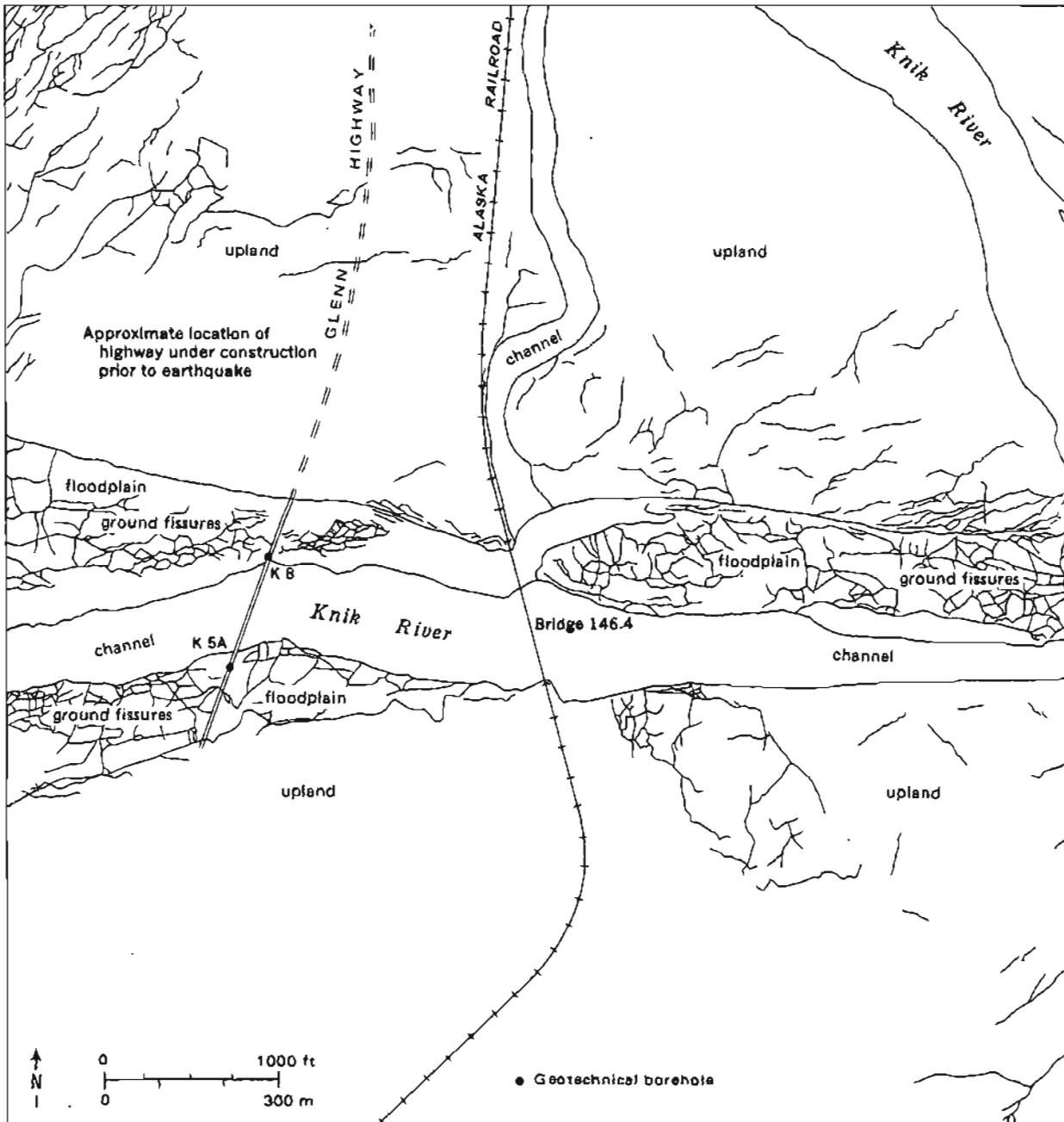


Figure 18. Map of distribution of ground fissures in the Knik River flood plain that resulted from the 1964 earthquake (McCulloch and Bonilla, 1970).

CPT curves suggest that the loose to slightly compact soils that correlate with similar soils at the material site occur to a depth of 20 to 30 ft (6 to 9 m) along most of the bridge centerline. By inference, the qualitative assessment of shallow liquefaction susceptibility extends to the foundation and abutment areas of the bridge. These foundation-study logs also indicate stratified gray sands and silts at depths of 60 ft (17 m) or more; these sands and silts are below the usual depth of liquefaction. However, according to the piling specifications (for the bridge piers), the piles were driven to about 46 ft (14 m), and the abutment piles were driven to 64 to 66 ft (19 to 20 m). Thus, liquefaction of these sands and silts could be an important factor for the static bearing strength of the support piles.

On the basis of these qualitative observations, I conclude that soils in the vicinity of the bridge are liquefiable within a zone from 4 to 30 ft (1 to 9 m) below ground surface, provided the soil is below the water table, which fluctuates significantly.

Standard-penetration-test Evaluation

If the criteria of depth, texture, and saturation are met, a more accurate assessment of liquefaction susceptibility can be derived from SPT data (N-values). Because the SPT is an in-situ method of empirically determining liquefaction susceptibility and relative density, several investigators have drawn correlations between N-values and liquefaction susceptibility. Nishiyama and others (1977) published a simple graph based on the relationship of depth, N-values, and observed liquefaction (fig. 19). Two data sets for the Knik River bridge were examined: 1) SPT values for which there is available soil-texture data from the Alaska Department of Transportation and Public Facilities foundation report (1963a), and 2) SPT-equivalent data, which were computer generated based on the CPT soundings and checked against the soil-behavior predictions in appendix A. When the resultant N-values vs depth were plotted on the Nishiyama diagram (fig. 19), there was no convincing evidence for liquefiable soils. However, a number of points lie within a 'questionable' intermediate domain, most at depths less than 35 ft (10.5 m) below ground surface. This diagram suggests that under saturated conditions, these soils could liquefy if subjected to severe cyclic-loading conditions during major earthquakes. Because the graph is not quantified based on factors such as ground-acceleration values or effective overburden pressures, the conclusion must remain generalized.

Quantitative Assessment

If sufficient in-situ characteristics of a sand deposit are known and assumptions are made on the level of cyclic earthquake-loading input, empirical correlations can be made with sand deposits that have liquefied during previous earthquakes. Seed and others (1983) refined this correlation and developed a methodology for applying the evaluation at a new site. Data available for the Knik River bridge are adequate for this approach.

Seed and others (1983) found that a convenient parameter for expressing the cyclic-liquefaction characteristics of a sand under level-ground conditions is the cyclic-stress ratio ($\tau_{av}/\bar{\sigma}_v$), where τ_{av} is the average

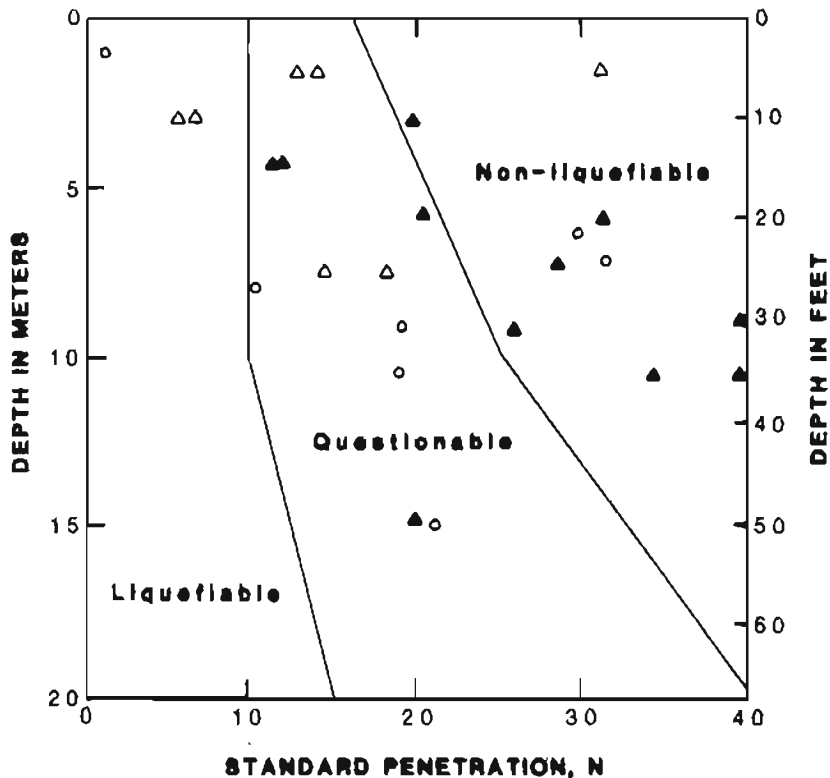


Figure 19. Plot of standard-penetration test (in blows/ft) vs depth showing domains of liquefaction susceptibility (modified from Nishiyama and others, 1977). Data points are from the Knik River bridge area, new Glenn Highway. Circles are actual SPT values, open triangles are silt/sand predicted by CPT, and solid triangles are sand predicted by CPT.

cyclic-shear stress developed on horizontal surfaces at any depth as a result of an assumed seismic loading, and σ_v is the initial vertical effective stress that acts on the sediment at that depth. Evaluation of this ratio requires data on sediment-layer characteristics and the intensity of cyclic loading. The relationships necessary to calculate the ratio are given in equations B-1 to B-4, appendix B.

Knowledge of the natural moisture content, dry density, wet density, particle-size distribution, sample depth, and soil stratigraphy are necessary to obtain the total vertical stress (σ_v) that acts on the subsurface sand horizon. Required calculations of σ_v are available in Lambe and Whitman (1979). Because the sand layers are below the water table (saturated), the pore-water pressure (U) must be computed and subtracted from σ_v to obtain the effective overburden pressure ($\bar{\sigma}_v$). The results of these calculations for the Knik River bridge site are given in table 1. The cyclic-stress-ratio equation (B-4, app. B) was calculated for sand horizons at depths of 60 ft (17 m) or less, assuming a static ground-water-table depth of 10 ft (3 m) and a maximum earthquake acceleration at the ground surface of 0.3 g.

The SPT blow-count information is used as a measure of relative density. Based on the work of Marcuson and Bieganousky (1976), a corrected penetration resistance (N_1) was proposed by Seed and others (1983) as B-6 (app. B); the resultant values are given in table 1.

Table 1. Data calculations for liquefaction-susceptibility analyses.

| Sample | Depth (ft) | σ_v (tsf) | $\bar{\sigma}_v$ (tsf) | $\sigma_v/\bar{\sigma}_v$ | r_d | $\tau_{av}/\bar{\sigma}_v$ | N (bpf) | C_N | N_1 (bpf) |
|--------|---------------|---------------------|---------------------------|---------------------------|-------|----------------------------|------------|-------|----------------|
| K5A-2 | 19 | 1.16 | 1.13 | 1.02 | 0.94 | 0.18 | 42 | 0.92 | 39 |
| K5A-3 | 21 | 1.29 | 0.95 | 1.36 | 0.93 | 0.25 | 30 | 0.86 | 26 |
| K5A-4 | 24 | 1.49 | 1.06 | 1.41 | 0.92 | 0.25 | 32 | 0.79 | 25 |
| K5A-5 | 26 | 1.63 | 1.13 | 1.44 | 0.91 | 0.25 | 11 | 0.74 | 8 |
| K5A-6 | 29 | 1.83 | 1.24 | 1.48 | 0.90 | 0.26 | 18 | 0.67 | 12 |
| K5A-8 | 34 | 2.17 | 1.42 | 1.53 | 0.89 | 0.27 | 18 | 0.58 | 10 |
| K5A-12 | 51 | 3.32 | 2.03 | 1.63 | 0.83 | 0.26 | 22 | 0.35 | 8 |
| K8-1 | 4 | 0.19 | 0.19 | 1.00 | 0.99 | 0.19 | 1.5 | 1.90 | 3 |
| K8-9 | 39 | 2.22 | 1.32 | 1.69 | 0.87 | 0.29 | 13 | 0.56 | 7 |
| K8-11 | 56 | 3.24 | 1.81 | 1.79 | 0.82 | 0.29 | 27 | 0.36 | 10 |
| K8-12 | 61 | 4.16 | 2.57 | 1.61 | 0.80 | 0.25 | 53 | 0.22 | 12 |

σ_v = total vertical stress

r_d = stress-reduction factor

N = SPT resistance

C_n = effective overburden function

$\bar{\sigma}_v$ = effective stress

τ_{av} = cyclic-stress ratio

N_1 = modified SPT resistance

tsf = tons/ft²

bpf = blows/ft²

On the basis of the above calculations and assumptions, the cyclic-stress ratio for 0.3 g peak ground acceleration is plotted against the modified penetration resistance (fig. 20). The boundary line on that graph (Seed and others, 1983) defines the transition from liquefiable to non-liquefiable soils for Richter magnitude 7.5 earthquakes on the basis of field observations and data collection from sites where liquefaction has occurred. Eight samples fall well within the liquefaction domain and show clustering that probably reflects the consistency of soil characteristics.

CONCLUSIONS

Immediately after the 1964 earthquake, the Knik River flood plain exhibited surface evidence of lateral spreading due to liquefaction of late

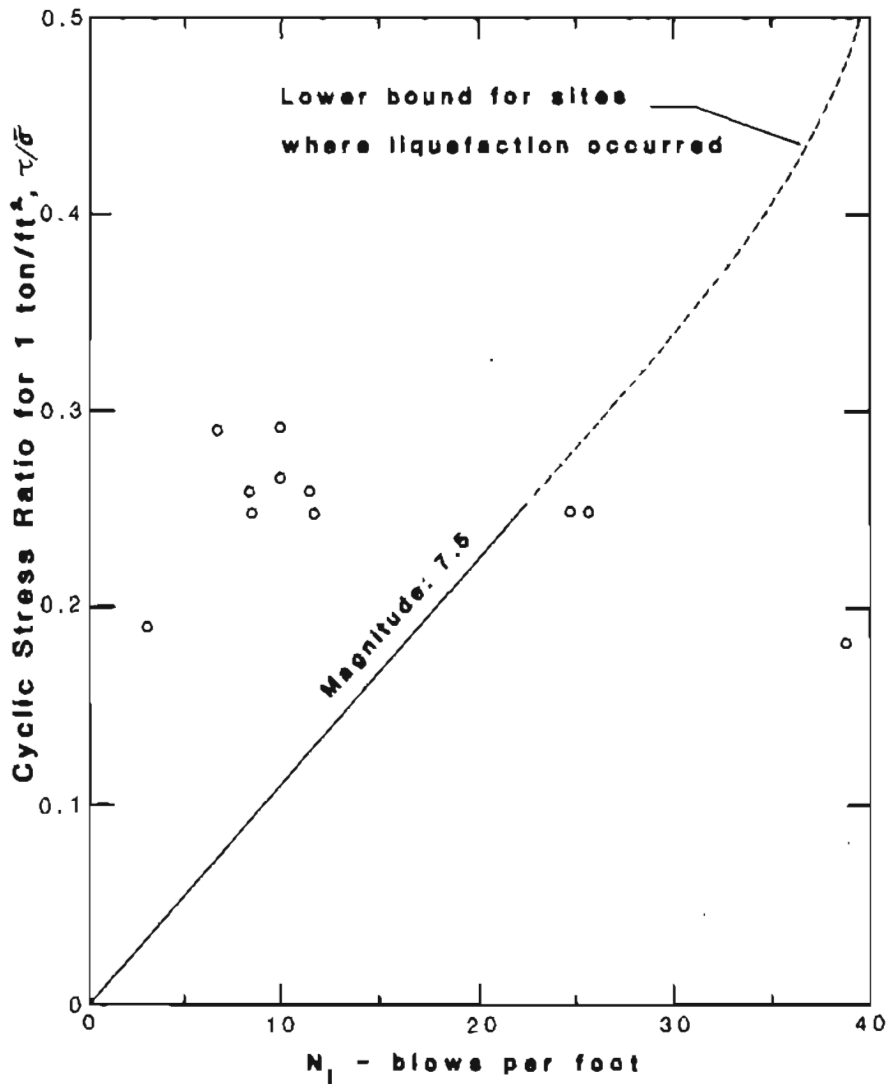


Figure 20. Plot of modified SPT blow count (N_1) vs cyclic-stress ratio (Seed and others, 1983). Points represent values calculated for Knik River bridge samples, assuming a peak surface-ground acceleration of 0.3 g. Note that eight values plot in the liquefiable domain and three values plot in the nonliquefiable domain.

Holocene fluvial deposits. Bridges sustained substantial damage that was at least partially due to instability of the foundation soils. On the basis of borehole data and the new CPT soundings, calculations were made using currently accepted methods of liquefaction-susceptibility analyses. The results of these calculations indicate that during major earthquakes, the foundation soils of the new Glenn Highway Knik River bridge are susceptible to liquefaction. This instability could have a serious affect on the integrity of the bridge. Although the design and configuration of the piles that support the piers and abutments would probably prevent total loss of the bridge, the structure could be rendered unusable for several months.

I am not aware of a means to increase the foundation stability at the site. Under static conditions, this bridge and others farther north over other channels of the Knik and Matanuska Rivers should perform safely and reliably for many years. Similarly, earthquakes of moderate magnitude should have little or no effect on these bridges. However, larger magnitude earthquakes---depending on their foci locations---are a serious concern for the integrity of these structures.

ACKNOWLEDGMENTS

This project was partially supported by the U.S. Geological Survey Office of Earthquake Studies (Agreement 14-08-001-A-0024). Personnel of Ertec Western, Inc., were essential to the success of this investigation. I also appreciate the technical data provided by the Alaska Department of Transportation and Public Facilities. Critical reviews of the manuscript by T.L. Youd (U.S. Geological Survey) and by R.A. Combellick and J.T. Kline (DGGs) are greatly appreciated.

REFERENCES CITED

- Alaska Department of Transportation and Public Facilities, 1963a, Foundation study report, Knik River and Matanuska River bridges: Anchorage, ADOT-PF Foundation Study Report Project F-042-1(7), 7 p.
- _____, 1963b, Materials report for Peters Creek to Palmer, Station 990+00 to 1127+00: Anchorage, ADOT-PF Materials Report Project F-042-1(7), 39 p.
- Begemann, H.K., 1965, The friction jacket cone as an aid in determining the soil profile: International Conference on Soil Mechanics and Foundation Engineering, 6th, Proceedings, v. 1, p. 17-20.
- Bennett, M.J., Youd, T.L., Harp, E.L., and Wieczorek, G.F., 1981, Subsurface investigation of liquefaction, Imperial Valley earthquake, California, October 15, 1979: U.S. Geological Survey Open-file Report 81-502, 83 p.
- Brown, L.D., Reilinger, R.E., Holdahl, S.R., and Balzaks, E.I., 1977, Postseismic crustal uplift near Anchorage, Alaska: Journal of Geophysical Research, v. 82, no. 4, p. 3369-3378.
- Casagrande, Arthur, 1976, Liquefaction and cyclic deformation of sands -- a critical review: Harvard University Soil Mechanics Series, no. 88, 51 p.
- Douglas, B.J., and Olsen, R.S., 1981, Soil classification using electric cone penetrometer: St. Louis, Missouri, American Society of Civil Engineers Special Technical Publication, 19 p.
- Douglas, B.J., Olsen, R.S., and Martin, G.R., 1981, Evaluation of the cone penetrometer tests for SPT-liquefaction assessment: American Society of Civil Engineers Preprint 81-544, 14 p.
- Ferritto, J.M., and Forrest, J.B., 1977, Determination of seismically induced liquefaction potential at proposed bridge sites, v. 1: Washington, D.C., Federal Highway Administration Report FHWA-RD-77-128, 130 p.
- Foster, H.L., and Karlstrom, T.N.V., 1967, Ground breakage and associated effects in the Cook Inlet area, Alaska, resulting from the March 27, 1964 earthquake: U.S. Geological Survey Professional Paper 543-F, p. F1-F28.

- Gibbs, H.J., and Holtz, W.G., 1957, Research on determining the density of sands by spoon penetration testing: International Conference on Soil Mechanics and Foundation Engineering, 4th, Proceedings, v. 1, p. 35-39.
- Kachadoorian, Reuben, 1968, Effects of the earthquake of March 27, 1964, on the Alaska highway system: U.S. Geological Survey Professional Paper 545-C, p. C1-C66.
- Lambe, T.W., and Whitman, R.V., 1979, Soil mechanics, SI version: New York, Wiley and Sons, 553 p.
- Marcuson, W.F., III, and Bieganousky, W.A., 1976, Laboratory standard penetration tests on fine sand: Journal of the Geotechnical Engineering Division, v. 103, no. G76, p. 565-588.
- McCulloch, D.S., and Bonilla, M.G., 1970, Effects of the earthquake of March 27, 1964, on the Alaska Railroad: U.S. Geological Survey Professional Paper 545-D, p. D1-D161.
- McLean, F.G., Franklin, A.G., and Dahlsrand, T.K., 1975, Influence of mechanical variables on the SPT: Conference on in-situ measurement of soil properties, Raleigh, North Carolina, 1975, Proceedings, v. 1, p. 287-318.
- Nishiyama, H., Yahagi, K., Nakagawa, S., and Wada, K., 1977, Practical method of predicting sand liquefaction: International Conference on Soil Mechanics and Foundation Engineering, 9th, Tokyo, Japan, 1977, Proceedings, v. 2, p. 305-308.
- Sanglerat, G., 1972, The penetrometer and soil exploration: New York, Elsevier, 488 p.
- Schmertmann, J.H., 1971, Discussion of the standard penetration test: Pan American Conference on Soil Mechanics and Foundation Engineering, 4th, San Juan, Puerto Rico, 1971, Proceedings, v. 3, p. 90-98.
- Searle, I.W., 1979, The interpretation of Begemann friction jacket cone results to give soil types and design parameters: ECSMFE, 7th, Brighton, England, 1979, Proceedings, v. 2, p. 265-70.
- Seed, H.B., 1968, Landslides during earthquakes due to soil liquefaction: Journal of the Soil Mechanics and Foundations Division, v. 94, no. SM5, p. 1053-1122.
- _____, 1976, Evaluation of soil liquefaction effects on level ground during earthquakes: American Society of Civil Engineers Specialty Session on Liquefaction Problems in Geotechnical Engineering, Philadelphia, 1975, Preprint 2752, p. 1-104.
- _____, 1979, Soil liquefaction and cyclic mobility evaluation for level ground during earthquakes: Journal of the Geotechnical Engineering Division, v. 105, no. GT2, p. 201-255.
- Seed, H.B., Idriss, I.M., and Arango, Ignacio, 1983, Evaluation of liquefaction potential using field performance data: Journal of the Geotechnical Engineering Division, v. 109, no. 3, p. 458-482.
- Sherif, M.A., and Ishibashi, J., 1978, Soil dynamics considerations for microzonation: International Conference on Microzonation, 2nd, San Francisco, 1978, Proceedings, v. 1, p. 81-110.
- Urdike, R.G., and Ulery, C.A., 1983, Preliminary geologic map of the Anchorage B-6 NW (Eklutna Lake) Quadrangle, Alaska: Alaska Division of Geological and Geophysical Surveys Report of Investigations 83-8, scale 1:10,000, 2 sheets.
- Youd, T.L., 1978, Major cause of earthquake damage is ground failure: Civil Engineering, v. 62, no. 2, p. 47-51.

- Youd, T.L., and Hoose, S.N., 1978, Historic ground failures in northern California associated with earthquakes: U.S. Geological Survey Professional Paper 993, 177 p.
- Youd, T.L., and Perkins, D.M., 1978, Mapping liquefaction-induced ground failure potential: Journal of the Geotechnical Engineering Division, v. 104, no. GT4, p. 433-446.

APPENDIX A

Tabulated data for cone-penetration-test soundings at the Knik River bridge, new Glenn Highway, Alaska.

Data recorded on the following tables include cone resistance, friction resistance, friction ratio, and soil-behavior-type predictions. These values are discussed in the text.

Table 2. CPT log for sounding KR-1.

| DEPTH FT | CONE TSF | FRICITION TSF | RATIO | SOIL BEHAVIOR TYPES |
|-------------|-------------|------------------|-------|-----------------------|
| 1.0 | 105.00 | 1.76 | 1.31 | SAND TO SILTY SAND |
| 2.0 | 177.70 | 1.45 | 1.16 | SAND TO SILTY SAND |
| 3.0 | 180.36 | 1.30 | 0.77 | SAND TO SILTY SAND |
| 4.0 | 87.01 | 1.20 | 1.59 | SAND TO SILTY SAND |
| 5.0 | 30.10 | 0.47 | 1.32 | SAND TO SILTY SAND |
| 6.0 | 142.77 | 0.91 | 0.79 | SAND TO SILTY SAND |
| 7.0 | 292.25 | 1.67 | 0.65 | GRAVELLY SAND TO SAND |
| 8.0 | 194.73 | 0.56 | 0.33 | GRAVELLY SAND TO SAND |
| 9.0 | 396.62 | 1.70 | 0.41 | GRAVELLY SAND TO SAND |
| 10.0 | 347.63 | 2.39 | 0.88 | SAND TO SILTY SAND |
| 11.0 | 298.03 | 2.69 | 0.80 | GRAVELLY SAND TO SAND |
| 12.0 | 214.41 | 1.82 | 0.88 | SAND TO SILTY SAND |
| 13.0 | 254.95 | 1.12 | 0.67 | GRAVELLY SAND TO SAND |
| 14.0 | 163.24 | 1.03 | 0.59 | SAND TO SILTY SAND |
| 15.0 | 190.78 | 0.73 | 0.52 | GRAVELLY SAND TO SAND |
| 16.0 | 192.96 | 1.27 | 0.65 | SAND TO SILTY SAND |
| 17.0 | 88.96 | 0.30 | 0.35 | SAND TO SILTY SAND |
| 18.0 | 111.91 | 0.88 | 0.91 | SAND TO SILTY SAND |
| 19.0 | 198.79 | 1.29 | 0.65 | SAND TO SILTY SAND |
| 20.0 | 124.33 | 0.49 | 0.46 | SAND TO SILTY SAND |
| 21.0 | 126.44 | 1.06 | 0.62 | SAND TO SILTY SAND |
| 22.0 | 130.46 | 0.70 | 0.56 | SAND TO SILTY SAND |
| 23.0 | 105.90 | 0.44 | 0.49 | SAND TO SILTY SAND |
| 24.0 | 78.39 | 0.64 | 0.72 | SAND TO SILTY SAND |
| 25.0 | 110.85 | 0.68 | 0.53 | SAND TO SILTY SAND |
| 26.0 | 131.63 | 0.44 | 0.39 | SAND TO SILTY SAND |
| 27.0 | 122.41 | 0.35 | 0.46 | SAND TO SILTY SAND |
| 28.0 | 148.37 | 1.00 | 0.55 | SAND TO SILTY SAND |
| 29.0 | 160.97 | 1.02 | 0.49 | SAND TO SILTY SAND |
| 30.0 | 224.31 | 1.28 | 0.58 | GRAVELLY SAND TO SAND |
| 31.0 | 89.71 | 1.06 | 1.10 | SAND TO SILTY SAND |
| 32.0 | 322.25 | 1.61 | 0.62 | GRAVELLY SAND TO SAND |
| 33.0 | 319.72 | 0.56 | 0.45 | GRAVELLY SAND TO SAND |
| 34.0 | 313.63 | 1.77 | 0.61 | GRAVELLY SAND TO SAND |
| 35.0 | 295.32 | 1.68 | 0.48 | GRAVELLY SAND TO SAND |
| 36.0 | 344.25 | 2.40 | 0.65 | GRAVELLY SAND TO SAND |
| 37.0 | 436.49 | 2.96 | 0.62 | GRAVELLY SAND TO SAND |
| 38.0 | 404.56 | 1.46 | 0.36 | GRAVELLY SAND TO SAND |
| 39.0 | 389.69 | 2.42 | 0.52 | GRAVELLY SAND TO SAND |
| 40.0 | 557.89 | 3.49 | 0.62 | GRAVELLY SAND TO SAND |
| 41.0 | 428.39 | 1.44 | 0.34 | GRAVELLY SAND TO SAND |
| 42.0 | 128.08 | 1.25 | 1.09 | SAND TO SILTY SAND |
| 43.0 | 89.41 | 1.33 | 1.48 | SAND TO SILTY SAND |
| 44.0 | 87.02 | 1.34 | 1.68 | SAND TO SILTY SAND |
| 45.0 | 348.56 | 1.49 | 0.49 | GRAVELLY SAND TO SAND |
| 46.0 | 164.95 | 1.50 | 0.76 | SAND TO SILTY SAND |
| 47.0 | 227.97 | 1.47 | 0.57 | GRAVELLY SAND TO SAND |
| 48.0 | 193.36 | 1.21 | 0.64 | SAND TO SILTY SAND |
| 49.0 | 126.75 | 0.64 | 0.68 | SAND TO SILTY SAND |
| 50.0 | 85.38 | 0.97 | 0.93 | SAND TO SILTY SAND |
| 51.0 | 80.27 | 0.44 | 0.55 | SAND TO SILTY SAND |
| 52.0 | 117.37 | 2.01 | 1.50 | SAND TO SILTY SAND |
| 53.0 | 318.74 | 2.44 | 0.75 | GRAVELLY SAND TO SAND |
| 54.0 | 300.81 | 2.59 | 0.75 | GRAVELLY SAND TO SAND |
| 55.0 | 482.97 | 1.38 | 0.40 | GRAVELLY SAND TO SAND |
| 56.0 | 269.78 | 2.57 | 0.94 | SAND TO SILTY SAND |
| 57.0 | 300.86 | 1.33 | 0.43 | GRAVELLY SAND TO SAND |
| 58.0 | 201.36 | 1.48 | 0.70 | SAND TO SILTY SAND |
| 59.0 | 280.13 | 1.31 | 0.58 | GRAVELLY SAND TO SAND |
| 60.0 | 194.06 | 5.61 | 2.62 | SAND TO SILTY SAND |
| 61.0 | 148.41 | 2.84 | 2.32 | SAND TO SILTY SAND |
| 62.0 | 100.48 | 2.59 | 2.81 | SAND TO SILTY SAND |
| 63.0 | 56.87 | 1.75 | 2.71 | SAND TO SILTY SAND |
| 64.0 | 33.94 | 1.17 | 3.56 | SAND TO SILTY SAND |
| 65.0 | 45.67 | 1.29 | 2.79 | SAND TO SILTY SAND |
| 66.0 | 55.36 | 1.19 | 2.63 | SAND TO SILTY SAND |
| 67.0 | 29.17 | 0.87 | 2.90 | SAND TO SILTY SAND |
| 68.0 | 21.08 | 0.92 | 3.84 | SAND TO SILTY SAND |
| 69.0 | 37.81 | 1.10 | 3.28 | SAND TO SILTY SAND |

Table 2 (con.)

| KR C-01 | | | | RATIO | SOIL BEHAVIOR TYPES |
|-------------|-------------|-----------------|------|--------------------------|---------------------|
| DEPTH FT | CONE TSF | FRICTION TSF | | | |
| 70.0 | 61.67 | 0.90 | 1.93 | SILTY SAND TO SANDY SILT | |
| 71.0 | 29.28 | 0.78 | 3.64 | SILTY CLAY | |
| 72.0 | 32.73 | 1.26 | 3.09 | SILTY CLAY | |
| 73.0 | 21.02 | 0.84 | 3.52 | SILTY CLAY TO CLAY | |
| 74.0 | 24.16 | 0.94 | 2.56 | SILTY CLAY | |
| 75.0 | 23.46 | 1.21 | 4.07 | SILTY CLAY TO CLAY | |
| 76.0 | 57.44 | 1.54 | 2.04 | SILTY SAND TO SANDY SILT | |
| 77.0 | 246.47 | 2.23 | 0.88 | SAND TO SILTY SAND | |
| 78.0 | 185.62 | 1.67 | 0.89 | SAND TO SILTY SAND | |
| 79.0 | 165.69 | 1.61 | 0.92 | SAND TO SILTY SAND | |
| 80.0 | 123.75 | 1.13 | 0.94 | SAND TO SILTY SAND | |
| 81.0 | 63.11 | 1.38 | 1.79 | SILTY SAND TO SANDY SILT | |
| 82.0 | 69.15 | 1.48 | 1.89 | SILTY SAND TO SANDY SILT | |
| 83.0 | 116.17 | 1.31 | 1.22 | SAND TO SILTY SAND | |
| 84.0 | 104.38 | 1.61 | 1.87 | SILTY SAND TO SANDY SILT | |
| 85.0 | 103.60 | 1.57 | 1.12 | SAND TO SILTY SAND | |
| 86.0 | 117.50 | 1.34 | 1.21 | SAND TO SILTY SAND | |
| 87.0 | 81.31 | 0.95 | 1.32 | SAND TO SILTY SAND | |
| 88.0 | 92.28 | 1.32 | 1.36 | SAND TO SILTY SAND | |
| 89.0 | 67.16 | 1.44 | 1.65 | SILTY SAND TO SANDY SILT | |
| 90.0 | 60.03 | 1.17 | 1.71 | SILTY SAND TO SANDY SILT | |
| 91.0 | 74.94 | 1.35 | 2.01 | SILTY SAND TO SANDY SILT | |
| 92.0 | 53.21 | 0.77 | 1.64 | SILTY SAND TO SANDY SILT | |
| 93.0 | 48.16 | 1.06 | 1.92 | SANDY SI TO CLAYEY SILT | |
| 94.0 | 93.23 | 1.25 | 1.32 | SAND TO SILTY SAND | |
| 95.0 | 169.14 | 1.55 | 0.95 | SAND TO SILTY SAND | |
| 96.0 | 124.36 | 1.35 | 1.12 | SAND TO SILTY SAND | |
| 97.0 | 158.24 | 1.68 | 1.08 | SAND TO SILTY SAND | |
| 98.0 | 179.24 | 2.10 | 1.14 | SAND TO SILTY SAND | |
| 99.0 | 188.78 | 2.14 | 1.14 | SAND TO SILTY SAND | |
| 100.0 | 234.47 | 2.65 | 1.13 | SAND TO SILTY SAND | |
| 101.0 | 224.43 | 2.16 | 0.97 | SAND TO SILTY SAND | |
| 102.0 | 205.10 | 2.17 | 0.92 | SAND TO SILTY SAND | |
| 103.0 | 169.73 | 2.53 | 1.39 | SAND TO SILTY SAND | |
| 104.0 | 51.15 | 1.46 | 2.40 | BANDY SI TO CLAYEY SILT | |
| 105.0 | 74.93 | 1.30 | 1.57 | SILTY SAND TO SANDY SILT | |
| 106.0 | 118.69 | 1.38 | 1.25 | SAND TO SILTY SAND | |
| 107.0 | 113.23 | 1.33 | 1.29 | SAND TO SILTY SAND | |
| 108.0 | 71.91 | 1.25 | 1.67 | SILTY SAND TO SANDY SILT | |
| 109.0 | 38.96 | 1.06 | 2.24 | SANDY SI TO CLAYEY SILT | |

Table 3. CPT log for sounding KR-2.

| DEPTH F1 | CONE TSF | FRICTION TSF | RATIO | SOIL BEHAVIOR TYPES |
|-------------|-------------|-----------------|-------|--------------------------|
| 1.0 | 183.72 | 3.13 | 1.97 | SILTY SA TO CLAYEY SAND |
| 2.0 | 343.94 | 3.10 | 1.02 | SAND TO SILTY SAND |
| 3.0 | 363.03 | 4.18 | 1.16 | SAND TO SILTY SAND |
| 4.0 | 194.13 | 1.73 | 1.34 | SAND TO SILTY SAND |
| 5.0 | 150.22 | 2.79 | 1.48 | SAND TO SILTY SAND |
| 6.0 | 204.00 | 2.72 | 1.69 | SAND TO SILTY SAND |
| 7.0 | 102.61 | 0.89 | 0.86 | SAND TO SILTY SAND |
| 8.0 | 41.48 | 0.42 | 1.18 | SILTY SAND TO SANDY SILT |
| 9.0 | 73.94 | 0.70 | 0.83 | SAND TO SILTY SAND |
| 10.0 | 51.20 | 0.70 | 1.23 | SILTY SAND TO SANDY SILT |
| 11.0 | 98.35 | 0.68 | 1.23 | SAND TO SILTY SAND |
| 12.0 | 92.41 | 0.92 | 0.99 | SAND TO SILTY SAND |
| 13.0 | 97.92 | 1.96 | 1.30 | SAND TO SILTY SAND |
| 14.0 | 119.22 | 0.45 | 0.72 | SAND TO SILTY SAND |
| 15.0 | 145.74 | 1.60 | 0.87 | SAND TO SILTY SAND |
| 16.0 | 251.36 | 2.98 | 0.80 | SAND TO SILTY SAND |
| 17.0 | 174.81 | 2.24 | 1.09 | SAND TO SILTY SAND |
| 18.0 | 238.39 | 1.81 | 0.87 | SAND TO SILTY SAND |
| 19.0 | 219.77 | 1.14 | 0.71 | SAND TO SILTY SAND |
| 20.0 | 143.53 | 0.91 | 0.57 | SAND TO SILTY SAND |
| 21.0 | 200.59 | 0.60 | 0.44 | GRAVELLY SAND TO SAND |
| 22.0 | 178.97 | 2.16 | 1.01 | SAND TO SILTY SAND |
| 23.0 | 304.87 | 2.78 | 0.66 | GRAVELLY SAND TO SAND |
| 24.0 | 306.01 | 2.19 | 0.54 | GRAVELLY SAND TO SAND |
| 25.0 | 372.81 | 3.00 | 0.80 | GRAVELLY SAND TO SAND |
| 26.0 | 270.07 | 1.39 | 0.59 | GRAVELLY SAND TO SAND |
| 27.0 | 197.07 | 1.86 | 0.93 | SAND TO SILTY SAND |
| 28.0 | 241.55 | 1.28 | 0.47 | GRAVELLY SAND TO SAND |
| 29.0 | 244.58 | 1.20 | 0.60 | GRAVELLY SAND TO SAND |
| 30.0 | 284.04 | 1.45 | 0.63 | GRAVELLY SAND TO SAND |
| 31.0 | 198.83 | 0.80 | 0.49 | GRAVELLY SAND TO SAND |
| 32.0 | 268.49 | 2.15 | 1.01 | SAND TO SILTY SAND |
| 33.0 | 283.81 | 1.51 | 0.49 | GRAVELLY SAND TO SAND |
| 34.0 | 311.61 | 2.38 | 0.69 | GRAVELLY SAND TO SAND |
| 35.0 | 304.65 | 1.73 | 0.78 | GRAVELLY SAND TO SAND |
| 36.0 | 303.65 | 1.20 | 0.48 | GRAVELLY SAND TO SAND |
| 37.0 | 145.97 | 1.04 | 0.71 | SAND TO SILTY SAND |
| 38.0 | 261.21 | 2.50 | 0.82 | SAND TO SILTY SAND |
| 39.0 | 190.81 | 1.07 | 0.63 | SAND TO SILTY SAND |
| 40.0 | 275.11 | 3.09 | 1.03 | SAND TO SILTY SAND |
| 41.0 | 262.35 | 1.23 | 0.44 | GRAVELLY SAND TO SAND |
| 42.0 | 200.62 | 1.48 | 0.73 | SAND TO SILTY SAND |
| 43.0 | 353.54 | 2.94 | 0.67 | GRAVELLY SAND TO SAND |
| 44.0 | 410.17 | 3.32 | 0.93 | SAND TO SILTY SAND |
| 45.0 | 270.57 | 0.70 | 0.39 | GRAVELLY SAND TO SAND |
| 46.0 | 146.48 | 0.88 | 0.60 | SAND TO SILTY SAND |
| 47.0 | 239.02 | 1.12 | 0.49 | GRAVELLY SAND TO SAND |
| 48.0 | 187.37 | 1.63 | 0.79 | SAND TO SILTY SAND |
| 49.0 | 222.95 | 1.68 | 0.74 | SAND TO SILTY SAND |
| 50.0 | 249.13 | 1.90 | 0.69 | GRAVELLY SAND TO SAND |
| 51.0 | 309.16 | 3.42 | 1.11 | SAND TO SILTY SAND |
| 52.0 | 446.67 | 2.37 | 0.60 | GRAVELLY SAND TO SAND |
| 53.0 | 499.90 | 3.59 | 0.81 | GRAVELLY SAND TO SAND |
| 54.0 | 367.91 | 2.03 | 0.65 | GRAVELLY SAND TO SAND |
| 55.0 | 320.45 | 1.40 | 0.57 | GRAVELLY SAND TO SAND |
| 56.0 | 314.70 | 1.88 | 0.56 | GRAVELLY SAND TO SAND |
| 57.0 | 383.99 | 1.86 | 0.56 | GRAVELLY SAND TO SAND |
| 58.0 | 276.59 | 1.22 | 0.47 | GRAVELLY SAND TO SAND |
| 59.0 | 401.62 | 3.22 | 0.81 | GRAVELLY SAND TO SAND |

Table 4. CPT log for sounding KR-3.

| DEPTH F1 | CONE TSF | FRICTION TSF | RATIO | SOIL BEHAVIOR TYPES |
|-------------|-------------|-----------------|-------|--------------------------|
| 1.0 | 395.18 | 7.72 | 1.68 | SAND TO SILTY SAND |
| 3.0 | 205.51 | 2.51 | 1.24 | SAND TO SILTY SAND |
| 4.0 | 154.04 | 2.01 | 1.36 | SAND TO SILTY SAND |
| 5.0 | 119.53 | 1.83 | 1.44 | SAND TO SILTY SAND |
| 6.0 | 61.65 | 1.42 | 2.24 | SANDY SI TO CLAYEY SILT |
| 7.0 | 67.98 | 1.53 | 2.15 | SILTY SAND TO SANDY SILT |
| 8.0 | 69.15 | 1.60 | 2.27 | CLAYEY SA TO SANDY CLAY |
| 9.0 | 75.67 | 1.41 | 1.88 | SILTY SAND TO SANDY SILT |
| 10.0 | 41.56 | 0.58 | 1.41 | SILTY SAND TO SANDY SILT |
| 11.0 | 35.42 | 0.55 | 1.85 | SANDY SI TO CLAYEY SILT |
| 12.0 | 41.50 | 0.51 | 1.41 | SILTY SAND TO SANDY SILT |
| 13.0 | 41.50 | 0.28 | 0.65 | SILTY SAND TO SANDY SILT |
| 14.0 | 36.90 | 0.28 | 0.73 | SILTY SAND TO SANDY SILT |
| 15.0 | 36.02 | 0.23 | 0.69 | SILTY SAND TO SANDY SILT |
| 16.0 | 52.72 | 0.35 | 0.65 | SAND TO SILTY SAND |
| 17.0 | 78.67 | 0.46 | 0.57 | SAND TO SILTY SAND |
| 18.0 | 74.57 | 0.43 | 0.54 | SAND TO SILTY SAND |
| 19.0 | 60.51 | 0.29 | 0.54 | SAND TO SILTY SAND |
| 20.0 | 62.30 | 0.89 | 1.40 | SILTY SAND TO SANDY SILT |
| 21.0 | 83.14 | 0.74 | 0.83 | SAND TO SILTY SAND |
| 22.0 | 80.42 | 0.50 | 0.60 | SAND TO SILTY SAND |
| 23.0 | 75.66 | 0.44 | 0.60 | SAND TO SILTY SAND |
| 24.0 | 78.75 | 0.46 | 0.61 | SAND TO SILTY SAND |
| 25.0 | 62.55 | 0.53 | 0.63 | SAND TO SILTY SAND |
| 26.0 | 44.98 | 0.92 | 2.14 | SANDY SI TO CLAYEY SILT |
| 27.0 | 106.41 | 0.71 | 0.67 | SAND TO SILTY SAND |
| 28.0 | 106.05 | 0.61 | 0.58 | SAND TO SILTY SAND |
| 29.0 | 92.90 | 0.81 | 0.89 | SAND TO SILTY SAND |
| 30.0 | 98.63 | 0.53 | 0.60 | SAND TO SILTY SAND |
| 31.0 | 91.88 | 0.63 | 0.68 | SAND TO SILTY SAND |
| 32.0 | 164.52 | 2.14 | 1.09 | SAND TO SILTY SAND |
| 33.0 | 212.00 | 1.23 | 0.49 | GRAVELLY SAND TO SAND |
| 34.0 | 220.16 | 1.47 | 0.54 | GRAVELLY SAND TO SAND |
| 35.0 | 137.47 | 1.00 | 0.71 | SAND TO SILTY SAND |
| 36.0 | 120.39 | 0.72 | 0.57 | SAND TO SILTY SAND |
| 37.0 | 189.56 | 1.09 | 0.70 | SAND TO SILTY SAND |
| 38.0 | 123.55 | 3.22 | 1.72 | SILTY SAND TO SANDY SILT |
| 39.0 | 310.24 | 1.41 | 0.61 | GRAVELLY SAND TO SAND |
| 40.0 | 134.32 | 0.80 | 0.66 | SAND TO SILTY SAND |
| 41.0 | 196.27 | 1.59 | 0.82 | SAND TO SILTY SAND |
| 42.0 | 256.75 | 1.52 | 0.71 | GRAVELLY SAND TO SAND |
| 43.0 | 243.49 | 1.28 | 0.57 | GRAVELLY SAND TO SAND |
| 44.0 | 138.94 | 0.64 | 0.48 | SAND TO SILTY SAND |
| 45.0 | 125.04 | 0.76 | 0.59 | SAND TO SILTY SAND |
| 46.0 | 185.53 | 1.28 | 0.65 | SAND TO SILTY SAND |
| 47.0 | 161.68 | 1.45 | 0.94 | SAND TO SILTY SAND |
| 48.0 | 157.60 | 1.00 | 0.66 | SAND TO SILTY SAND |
| 49.0 | 149.23 | 0.99 | 0.57 | SAND TO SILTY SAND |
| 50.0 | 137.50 | 1.32 | 0.92 | SAND TO SILTY SAND |
| 51.0 | 138.58 | 1.16 | 0.83 | SAND TO SILTY SAND |
| 52.0 | 146.31 | 0.97 | 0.66 | SAND TO SILTY SAND |
| 53.0 | 177.90 | 1.52 | 0.79 | SAND TO SILTY SAND |
| 54.0 | 357.31 | 3.09 | 0.77 | GRAVELLY SAND TO SAND |
| 55.0 | 219.21 | 2.23 | 0.77 | SAND TO SILTY SAND |
| 56.0 | 336.80 | 1.16 | 0.48 | GRAVELLY SAND TO SAND |
| 57.0 | 304.00 | 1.49 | 0.62 | SAND TO SILTY SAND |
| 58.0 | 158.66 | 2.53 | 1.28 | SAND TO SILTY SAND |
| 59.0 | 184.29 | 0.97 | 0.61 | SAND TO SILTY SAND |
| 60.0 | 167.79 | 2.51 | 1.18 | SAND TO SILTY SAND |

Table 5. CPT log for sounding KR-4.

| DEPTH FT | CONE TSF | FRICTION TSF | RATIO | SOIL BEHAVIOR TYPES |
|-------------|-------------|-----------------|-------|--------------------------|
| 1.0 | 594.68 | 5.72 | 1.13 | SAND TO SILTY SAND |
| 2.0 | 190.95 | 1.89 | 1.09 | SAND TO SILTY SAND |
| 3.0 | 124.09 | 1.47 | 1.14 | SAND TO SILTY SAND |
| 4.0 | 38.67 | 1.04 | 2.20 | SANDY SI TO CLAYEY SILT |
| 5.0 | 39.73 | 0.75 | 1.88 | SANDY SI TO CLAYEY SILT |
| 6.0 | 66.30 | 0.68 | 1.83 | SILTY SAND TO SANDY SILT |
| 7.0 | 33.63 | 0.60 | 2.00 | SANDY SI TO CLAYEY SILT |
| 8.0 | 27.27 | 0.56 | 1.95 | SANDY SI TO CLAYEY SILT |
| 9.0 | 22.87 | 0.48 | 2.06 | SANDY SI TO CLAYEY SILT |
| 10.0 | 28.46 | 0.53 | 1.81 | SANDY SI TO CLAYEY SILT |
| 11.0 | 21.44 | 0.40 | 1.96 | SANDY SI TO CLAYEY SILT |
| 12.0 | 23.99 | 0.32 | 2.16 | SILTY CLAY |
| 13.0 | 37.10 | 0.55 | 1.06 | SILTY SAND TO SANDY SILT |
| 14.0 | 48.96 | 0.43 | 0.93 | SILTY SAND TO SANDY SILT |
| 15.0 | 49.08 | 0.56 | 1.21 | SILTY SAND TO SANDY SILT |
| 16.0 | 47.09 | 0.85 | 1.78 | SILTY SAND TO SANDY SILT |
| 17.0 | 35.70 | 0.72 | 1.99 | SANDY SI TO CLAYEY SILT |
| 18.0 | 40.03 | 0.73 | 1.84 | SANDY SI TO CLAYEY SILT |
| 19.0 | 38.74 | 0.69 | 1.77 | SANDY SI TO CLAYEY SILT |
| 20.0 | 34.14 | 0.68 | 2.01 | SANDY SI TO CLAYEY SILT |
| 21.0 | 35.62 | 0.68 | 1.79 | SANDY SI TO CLAYEY SILT |
| 22.0 | 33.53 | 0.44 | 1.32 | SILTY SAND TO SANDY SILT |
| 23.0 | 28.67 | 0.63 | 2.80 | SILTY CLAY |
| 24.0 | 64.36 | 1.22 | 1.88 | SILTY SAND TO SANDY SILT |
| 25.0 | 50.99 | 0.91 | 1.95 | SANDY SI TO CLAYEY SILT |
| 26.0 | 53.70 | 0.95 | 1.68 | SILTY SAND TO SANDY SILT |
| 27.0 | 70.74 | 0.42 | 0.65 | SAND TO SILTY SAND |
| 28.0 | 72.31 | 0.36 | 0.48 | SAND TO SILTY SAND |
| 29.0 | 46.81 | 0.24 | 0.32 | SAND TO SILTY SAND |
| 30.0 | 102.96 | 0.57 | 0.55 | SAND TO SILTY SAND |
| 31.0 | 195.62 | 1.41 | 0.65 | SAND TO SILTY SAND |
| 32.0 | 202.57 | 1.09 | 0.52 | GRAVELLY SAND TO SAND |
| 33.0 | 235.23 | 2.23 | 0.76 | SAND TO SILTY SAND |
| 34.0 | 146.79 | 0.92 | 0.61 | SAND TO SILTY SAND |
| 35.0 | 117.38 | 0.39 | 0.46 | SAND TO SILTY SAND |
| 36.0 | 171.71 | 0.64 | 0.46 | GRAVELLY SAND TO SAND |
| 37.0 | 199.04 | 1.20 | 0.63 | SAND TO SILTY SAND |
| 38.0 | 161.71 | 1.48 | 0.97 | SAND TO SILTY SAND |
| 39.0 | 219.77 | 1.41 | 0.65 | GRAVELLY SAND TO SAND |
| 40.0 | 209.95 | 1.77 | 0.79 | SAND TO SILTY SAND |
| 41.0 | 209.04 | 0.84 | 0.52 | GRAVELLY SAND TO SAND |
| 42.0 | 198.61 | 0.87 | 0.43 | GRAVELLY SAND TO SAND |
| 43.0 | 229.46 | 1.07 | 0.47 | GRAVELLY SAND TO SAND |
| 44.0 | 195.52 | 2.95 | 0.87 | SAND TO SILTY SAND |
| 45.0 | 245.56 | 0.71 | 0.42 | GRAVELLY SAND TO SAND |
| 46.0 | 227.87 | 2.35 | 0.89 | SAND TO SILTY SAND |
| 47.0 | 363.23 | 2.19 | 0.65 | GRAVELLY SAND TO SAND |
| 48.0 | 262.16 | 2.44 | 0.76 | SAND TO SILTY SAND |
| 49.0 | 147.10 | 0.78 | 0.52 | SAND TO SILTY SAND |
| 50.0 | 224.51 | 1.78 | 0.84 | SAND TO SILTY SAND |
| 51.0 | 310.70 | 2.22 | 0.68 | GRAVELLY SAND TO SAND |
| 52.0 | 358.82 | 2.50 | 0.59 | GRAVELLY SAND TO SAND |
| 53.0 | 381.91 | 2.00 | 0.52 | GRAVELLY SAND TO SAND |
| 54.0 | 300.55 | 2.95 | 1.01 | SAND TO SILTY SAND |
| 55.0 | 198.15 | 0.75 | 0.53 | GRAVELLY SAND TO SAND |
| 56.0 | 129.05 | 2.43 | 1.59 | SAND TO SILTY SAND |
| 57.0 | 198.47 | 2.38 | 0.80 | SAND TO SILTY SAND |
| 58.0 | 330.78 | 2.52 | 0.70 | GRAVELLY SAND TO SAND |
| 59.0 | 360.81 | 1.65 | 0.47 | GRAVELLY SAND TO SAND |

APPENDIX B
Equations used for calculations.

B-1 Total vertical stress, $\sigma_v = \Sigma[\Delta Z \times \gamma_t]$ where ΔZ = thickness of soil increment and γ_t = total unit weight of soil increment

B-2 Pore water pressure, $U = \Sigma[\Delta Z_w \times \gamma_w]$ where ΔZ_w = thickness of saturated soil increment and γ_w = unit weight of water

B-3 Total effective stress, $\bar{\sigma}_v = \sigma_v - U$

B-4 Cyclic-stress ratio, $\tau_{av} / \bar{\sigma}_v = 0.65 \times a_{\max}/g \times \sigma_v / \bar{\sigma}_v \times r_d$
where $a_{\max}/g = 0.30 g$
and r_d = stress-reduction factor (Seed and Idriss, 1981)

B-5 Effective overburden function, $C_N = 1 - 1.25 \log \bar{\sigma}_v$
where $\bar{\sigma}_v$ = total effective stress

B-6 Modified standard penetration resistance,

$$N_1 = C_N \times N$$

where N = field standard penetration resistance, in blows/ft